

# Consistent Community Detection in Continuous-Time Networks of Relational Events

**Makan Arastuie**

MAKAN.ARASTUIE@ROCKETS.UTOLEDO.EDU

*Department of Electrical Engineering and Computer Science*

*University of Toledo*

*Toledo, OH 43606, USA*

**Subhadeep Paul**

PAUL.963@OSU.EDU

*Department of Statistics*

*The Ohio State University*

*Columbus, OH 43210, USA*

**Kevin S. Xu**

KEVIN.XU@UTOLEDO.EDU

*Department of Electrical Engineering and Computer Science*

*University of Toledo*

*Toledo, OH 43606, USA*

## Abstract

In many application settings involving networks, such as messages between users of an on-line social network or transactions between traders in financial markets, the observed data are in the form of relational events with timestamps, which form a continuous-time network. We propose the *Community Hawkes Independent Pairs (CHIP)* model for community detection on such timestamped relational event data. We demonstrate that applying spectral clustering to adjacency matrices constructed from relational events generated by the CHIP model provides *consistent community detection* for a growing number of nodes. In particular, we obtain explicit non-asymptotic upper bounds on the misclustering rates based on the separation conditions required on the parameters of the model for consistent community detection. We also develop consistent and computationally efficient estimators for the parameters of the model. We demonstrate that our proposed CHIP model and estimation procedure scales to large networks with tens of thousands of nodes and provides superior fits compared to existing continuous-time network models on several real networks.

**Keywords:** dynamic network model, point process network model, event-based network, stochastic block model, spectral clustering, consistent estimation, Hawkes process

## 1. Introduction

A variety of complex systems in the computer, information, biological, and social sciences can be represented as a network, which consists of a set of objects (nodes) and relationships (edges) between the nodes. In many application settings, we observe not just the presence or absence of edges between nodes, but also distinct events occurring between nodes over time. For example, in on-line social networks, users interact with each other through events that occur at specific time instances such as liking, mentioning, tagging, or sharing another user's content. Such interactions form *timestamped relational events*, which define a dynamic network that is continuously evolving over time.

Sender	Receiver	Time
1	2	0.1
2	3	0.4
1	3	0.6
3	1	0.8
1	2	0.9
4	2	1.3
2	3	1.5
1	2	1.8

$$N = \begin{bmatrix} 0 & 3 & 1 & 0 \\ 0 & 0 & 2 & 0 \\ 1 & 0 & 0 & 0 \\ 0 & 1 & 0 & 0 \end{bmatrix}$$

(b) Weighted adjacency matrix

$$A = \begin{bmatrix} 0 & 1 & 1 & 0 \\ 0 & 0 & 1 & 0 \\ 1 & 0 & 0 & 0 \\ 0 & 1 & 0 & 0 \end{bmatrix}$$

(c) Adjacency matrix

(a) Event table

Figure 1: Three representations of a continuous-time network of timestamped relational events. The weighted adjacency matrix representation discards the timestamps and ordering of events. The (unweighted) adjacency matrix representation further discards the number of occurrences of events.

Relational event data are typically presented in the form of an event table, as shown in Figure 1a. An event table can be mathematically represented by an  $l \times 3$  event matrix  $Y$ , where each row is a triplet  $(i, j, t)$  denoting an event from node  $i$  (sender) to node  $j$  (receiver) at timestamp  $t$ , and  $l$  denotes the number of events. From an event table, we can also extract a weighted adjacency matrix  $N$ , shown in Figure 1b, by counting the number of events occurring between node pairs over the entire duration, and an unweighted or binary adjacency matrix  $A$ , shown in Figure 1c.

A variety of statistical models for such relational event data have recently appeared in the literature (DuBois and Smyth, 2010; Blundell et al., 2012; DuBois et al., 2013; Xin et al., 2017; Matias et al., 2018; Fox et al., 2016; Yang et al., 2017; Junuthula et al., 2019). These models, which we refer to as *continuous-time network models*, typically combine a point process model for the event times with a network model for the sender and receiver. They provide a low-dimensional representation of a continuous-time network that can be used for a variety of tasks including exploratory analysis and prediction of future events. For relational event data, continuous-time network models are often superior to their discrete-time counterparts (Xing et al., 2010; Yang et al., 2011; Xu and Hero III, 2014; Xu, 2015; Matias and Miele, 2017), which first aggregate events over time windows to form discrete-time network “snapshots” and thus lose granularity in modeling temporal dynamics.

Junuthula et al. (2019) recently proposed a Block Hawkes Model (BHM) for relational event data, inspired by the Stochastic Block Model (SBM) for static networks (Holland et al., 1983). However, the BHM introduces a dependency between pairs of nodes in the same community, which makes it difficult to analyze. Inspired by the BHM, we propose the *Community Hawkes Independent Pairs (CHIP)* model where pairs of nodes in the same community generate events according to independent univariate Hawkes processes with shared parameters, so that the number of parameters remains the same as in the BHM. However, the independence between node pairs enables tractable analysis of the CHIP model, unlike the BHM.

Our main contributions are as follows:

- We demonstrate that spectral clustering provides consistent community detection in the CHIP model for a growing number of nodes.
- We propose a consistent and computationally efficient estimator for the model parameters for a growing number of nodes and time duration.
- We show that the CHIP model provides better fits to several real data sets and scales to much larger networks than existing models, including a Facebook wall post network with  $> 40,000$  nodes and  $> 800,000$  events.

Other point process network models have demonstrated good empirical results, but to the best of our knowledge, this work provides the first theoretical guarantee of estimation accuracy for a point process network model. We believe that our asymptotic analysis also has tremendous practical value given the excellent scalability of our model to large networks with tens of thousands of nodes. The scalability of our methods enables us to understand interaction patterns in Facebook wall post data and detect communities with diverse characteristics of communication patterns over time beyond the usual strong intra-community and weak inter-community connections.

## 2. Background

We begin with a brief introduction to the Hawkes process and the stochastic block model, which form the main building blocks to our proposed CHIP model. We then discuss related work on point process models for networks.

### 2.1 Hawkes Processes

The Hawkes process, first introduced by Hawkes (1971b), is a counting process designed to model continuous-time arrivals of events that naturally cluster together in time, where the arrival of an event increases the chance of the next event arrival immediately after. Therefore, Hawkes processes have been used to model events in a variety of application settings including earthquakes (Marsan and Lengline, 2008), financial markets (Embrechts et al., 2011; Bacry et al., 2015), and social media (Simma and Jordan, 2012; DuBois et al., 2013; Zhou et al., 2013; Rizoïu et al., 2017).

A univariate Hawkes process is a *self-exciting* point process where its conditional intensity function given a sequence of event arrival times  $\{t_1, t_2, t_3, \dots, t_l\}$  for  $l$  events up to time duration  $T$  takes the general form:

$$\lambda(t) = \mu + \sum_{t_i < t}^{t_l} \gamma(t - t_i),$$

where  $\mu$  is the background intensity and  $\gamma(\cdot)$  is the kernel or the excitation function. A frequent choice of excitation function is an exponential kernel, which has been shown to provide a good fit for relational event data in social media (Halpin and De Boeck, 2013; Masuda et al., 2013; Zhao et al., 2015; Junuthula et al., 2019). Thus, we consider an exponential kernel for the CHIP model throughout this paper.  $\gamma(\cdot)$  is then parameterized

by  $\alpha, \beta > 0$  as follows:

$$\lambda(t) = \mu + \sum_{t_i < t}^{t_l} \alpha e^{-\beta(t-t_i)},$$

where the arrival of an event instantaneously increases the conditional intensity of the point process by  $\alpha$ , also called the jump size, at which point the intensity decays exponentially back towards  $\mu$ , at rate  $\beta$ . We restrict  $\alpha < \beta$ , so that the process is stationary.

Ozaki (1979) derived the log-likelihood function for Hawkes processes with exponential kernels, which takes the form:

$$\log \mathcal{L} = -\mu T + \sum_{q=1}^l \frac{\alpha}{\beta} \{e^{-\beta(T-t_q)} - 1\} + \sum_{q=1}^l \log(\mu + \alpha w(q)) \quad (1)$$

where  $w(q) = \sum_{q': t_{q'} < t_q} e^{-\beta(t_q - t_{q'})}$ . Moreover,  $w(q)$  can be computed recursively using  $w(q) = e^{-\beta(t_q - t_{q-1})}(1 + w(q-1))$ , with the added base case of  $w(1) = 0$ , which drops the double summation in the last term and decreases the computational complexity of the log-likelihood from  $\mathcal{O}(l^2)$  to  $\mathcal{O}(l)$  (Laub et al., 2015). The three parameters  $\mu, \alpha, \beta$  can be estimated by maximizing (1) using standard numerical methods for non-linear optimization (Nocedal and Wright, 2006).

## 2.2 The Stochastic Block Model

Most statistical models for networks consider a static network rather than a network of relational events. Many commonly used models of this type are discussed in the survey by Goldenberg et al. (2010). A static network with  $n$  nodes can be represented by an  $n \times n$  adjacency matrix  $A$  where  $A_{ij} = 1$  if there is an edge between nodes  $i$  and  $j$  and  $A_{ij} = 0$  otherwise. We consider networks with no self-edges, so  $A_{ii} = 0$  for all  $i$ . In the case of a directed network, we let  $A_{ij} = 1$  if there is an edge from node  $i$  to node  $j$ .

One model that has received significant attention is the *stochastic block model* (SBM), formalized by Holland et al. (1983). In the SBM, every node  $i$  is assigned to one and only one community or *block*  $c_i \in \{1, \dots, k\}$ , where  $k$  denotes the total number of blocks. Given the block membership vector  $\mathbf{c} = [c_i]_{i=1}^n$ , all entries of the adjacency matrix  $A_{ij}$  are independent. Additionally, for any nodes  $i \neq j$  and  $i' \neq j'$ , if  $i$  and  $i'$  are in the same block, i.e.  $c_i = c_{i'}$ , and  $j$  and  $j'$  are in the same block, i.e.  $c_j = c_{j'}$ , then  $A_{ij}$  and  $A_{i'j'}$  are identically distributed. Thus the probability of forming an edge between nodes  $i$  and  $j$  depends only on the block memberships  $c_i$  and  $c_j$ .

There have been significant recent advancements in the analysis of estimators for the static SBM. In particular, several variants of spectral clustering (Von Luxburg, 2007) have been shown to be consistent estimators of the community assignments for a growing number of nodes (Rohe et al., 2011; Sussman et al., 2012; Qin and Rohe, 2013; Lei and Rinaldo, 2015; Chin et al., 2015; Gao et al., 2017; Vu, 2018). Spectral clustering scales to large networks with tens of thousands of nodes and is generally not sensitive to initialization so it is also a practically useful estimator. The spectral clustering algorithm for directed networks that we consider in this paper is shown in Algorithm 1.

---

**Algorithm 1:** Spectral clustering algorithm for community detection in directed networks

---

**Input:** Adjacency Matrix  $A$ , number of blocks  $k$

**Result:** Estimated block assignments  $\hat{C}$

- 1 Compute singular value decomposition of  $A$ ;
  - 2  $\hat{\Sigma} \leftarrow$  diagonal matrix of  $k$  largest singular values of  $A$ ;
  - 3  $\hat{U}, \hat{V} \leftarrow$  left and right singular vectors of  $A$  corresponding to  $k$  largest singular values;
  - 4  $\hat{Z} \leftarrow$  concatenate( $\hat{U}, \hat{V}$ );
  - 5 Normalize the magnitude of each row of  $\hat{Z}$  to 1;
  - 6  $\hat{C} \leftarrow$  k-means clustering on rows of  $\hat{Z}$ ;
  - 7 **return**  $\hat{C}$
- 

### 2.3 Related Work

Point process models for networks, typically involving Hawkes processes, have been used in two main settings. The first setting involves estimating the structure of a latent or unobserved network from observed events at the nodes (Linderman and Adams, 2014, 2015; Farajtabar et al., 2015; Tran et al., 2015; He et al., 2015; Hall and Willett, 2016). These models are often used to estimate static networks of diffusion from information cascades, which often consist of a set of events of the form  $(i, t)$  denoting that node  $i$  performed an event of interest, e.g. a post on social media or a purchase of a product, at timestamp  $t$ .

In the second setting, which we consider in this paper, we directly observe events *between pairs of nodes* so that events take on the form  $(i, j, t)$  denoting an event from node  $i$  to node  $j$  at timestamp  $t$ . Our objective is to model the dynamics of such relational event sequences. In many applications, including networks of messages on on-line social networks, most pairs of nodes either never or rarely interact and thus have no events or very few events between them. Thus, most prior work in this setting utilizes low-dimensional latent variable representations of the networks to parameterize the point processes. The latent variable representations are often inspired by generative models for static networks such as continuous latent space models (Hoff et al., 2002) and stochastic block models (Holland et al., 1983), resulting in the development of point process network models with continuous latent space representations (Yang et al., 2017) and latent block or community representations (DuBois and Smyth, 2010; Blundell et al., 2012; DuBois et al., 2013; Xin et al., 2017; Matias et al., 2018; Junuthula et al., 2019). Point process network models with latent community representations are most closely related to the model we consider in this paper, and we discuss several of them in greater detail in Section 3.1.

Exact inference in point process network models with latent communities is usually intractable due to the discrete nature of the community assignments. Thus, prior work has typically utilized Markov Chain Monte Carlo (MCMC) (Blundell et al., 2012; DuBois et al., 2013) or variational inference (Matias et al., 2018; Junuthula et al., 2019) for approximate inference. While such approaches have demonstrated good empirical results, to the best of our knowledge, they come with no theoretical guarantees.

Junuthula et al. (2019) showed that there is an asymptotic equivalence between the block Hawkes model they proposed and the SBM and used this equivalence to motivate

an estimation procedure using spectral clustering followed by a local search, which they found to perform well in practice compared to mean-field variational inference. However, they also did not provide any theoretical guarantees despite demonstrating the asymptotic equivalence to the SBM.

### 3. The Community Hawkes Independent Pairs Model

We define a generative model for relational event networks that we call the *Community Hawkes Independent Pairs (CHIP)* model with parameters  $(\boldsymbol{\pi}, \mu, \alpha, \beta)$  as follows. Each node is assigned to a community or block  $a \in \{1, \dots, k\}$  with probability  $\pi_a$ , where each entry of  $\boldsymbol{\pi}$  is non-negative and all entries sum to 1. We represent the block assignments of all nodes either by a length  $n$  vector  $\mathbf{c} = [c_i]_{i=1}^n$  or an  $n \times k$  binary matrix  $C$  where  $c_i = k$  is equivalent to  $C_{ik} = 1$ ,  $C_{iq} = 0$  for all  $q \neq k$ . Each of the parameters  $\mu, \alpha, \beta$  is a  $k \times k$  matrix. Event times between node pairs  $(i, j)$  within a block pair  $(a, b)$  follow independent exponential Hawkes processes with shared parameters: baseline rate  $\mu_{ab}$ , jump size  $\alpha_{ab}$ , and decay rate  $\beta_{ab}$ . The generative process for our proposed CHIP model is as follows:

$$\begin{aligned} c_i &\sim \text{Categorical}(\boldsymbol{\pi}) && \text{for all } i \in \{1, \dots, n\} \\ \mathbf{t}_{ij} &\sim \text{Hawkes process}(\mu_{c_i c_j}, \alpha_{c_i c_j}, \beta_{c_i c_j}) && \text{for all } i, j \in \{1, \dots, n\}, i \neq j \\ Y &= \text{Row concatenate } [(i\mathbf{1}, j\mathbf{1}, \mathbf{t}_{ij})] && \text{over all } i, j \in \{1, \dots, n\}, i \neq j \end{aligned}$$

Let  $T$  denote the end time of the Hawkes process, which would correspond to the duration of the data trace. The column vector of event times  $\mathbf{t}_{ij}$  has length  $N_{ij}(T)$ , which denotes the number of events from node  $i$  to node  $j$  up to time  $T$ .  $Y$  denotes the event matrix and has dimensions  $l \times 3$ , where  $l = \sum_{i,j} N_{ij}(T)$  denotes the total number of observed events over all node pairs. It is constructed by row concatenating triplets  $(i, j, t_{ij}(q))$  over all events  $q \in \{1, \dots, N_{ij}(T)\}$  for all node pairs  $i, j \in \{1, \dots, n\}, i \neq j$ .

#### 3.1 Relation to Other Models

Our proposed CHIP model has a generative structure inspired by the SBM for static networks. Other point process network models in the literature have also utilized similar block structures (DuBois and Smyth, 2010; Blundell et al., 2012; DuBois et al., 2013; Xin et al., 2017; Matias et al., 2018; Junuthula et al., 2019). Within these models, the block structures have been incorporated in two different approaches.

One approach involves placing point process models at the level of block pairs (Blundell et al., 2012; Xin et al., 2017; Matias et al., 2018; Junuthula et al., 2019). For a network with  $k$  blocks,  $k^2$  different point processes are used to generate events between the  $k^2$  block pairs. To generate events between actual pairs of nodes, rather than pairs of blocks, the point processes are thinned by randomly selecting nodes from the respective blocks so that all nodes in a block are stochastically equivalent, in the spirit of the stochastic block model. The Block Hawkes Model (BHM) of Junuthula et al. (2019) follows this structure and uses exponential Hawkes processes to generate events between block pairs. The random assignment or thinning converts the univariate Hawkes process for a particular block pair  $(a, b)$  into a multivariate Hawkes process with  $n_{ab}$  dependent variables representing each of

---

**Algorithm 2:** Estimation procedure for Community Hawkes Independent Pairs model

---

**Input:** Relational event matrix  $Y$ , number of blocks  $k$   
**Result:** Estimated block assignments  $\hat{C}$  and Hawkes process parameters  $\hat{\mu}, \hat{\alpha}, \hat{\beta}$

- 1 **forall** *node pairs*  $i \neq j$  **do**
- 2 |  $N_{ij}$  = number of events from  $i$  to  $j$  in event matrix  $Y$ ;
- 3 **end**
- 4  $\hat{C} \leftarrow$  Spectral clustering( $N, k$ ) *or*  $\hat{C} \leftarrow$  Spectral clustering( $A, k$ );
- 5 **forall** *block pairs*  $(a, b)$  **do**
- 6 |  $\hat{m}_{ab} \leftarrow 1 - \sqrt{\frac{\bar{N}_{ab}}{S_{ab}^2}}$ ; // see equations (2) and (3) for details
- 7 |  $\hat{\mu}_{ab} \leftarrow \frac{1}{T} \sqrt{\frac{(\bar{N}_{ab})^3}{S_{ab}^2}}$ ;
- 8 |  $\hat{\beta}_{ab} \leftarrow$  maximizer of log-likelihood (6) using scalar optimization;
- 9 |  $\hat{\alpha}_{ab} \leftarrow \hat{\beta}_{ab} \hat{m}_{ab}$ ;
- 10 **end**
- 11 **return**  $[\hat{C}, \hat{\mu}, \hat{\alpha}, \hat{\beta}]$

---

the  $n_{ab}$  node pairs in the block pair. While such models have demonstrated good empirical results, the dependency between node pairs complicates analysis of the models.

The other approach involves modeling pairs of nodes with independent point processes that share parameters among nodes in the same block (DuBois and Smyth, 2010; DuBois et al., 2013). By having node pairs in the same block share parameters, the number of parameters is the same as for the models that place point process at the level of block pairs. However, by using independent point processes for all node pairs, there is no dependency between node pairs, which simplifies analysis of the model. We exploit this independence to perform the asymptotic analysis in Section 4. The disadvantage of using independent Hawkes processes for different node pairs is that it does not enable events between a node pair to affect the probability of events between other node pairs. Despite this disadvantage, we demonstrate in Section 5.2 that our proposed CHIP is able to achieve better fits to several real networks compared to other models.

### 3.2 Estimation Procedure

Our observed data consists of the event matrix  $Y$  containing the sender, receiver, and timestamp of each event. From  $Y$ , we need to jointly estimate the block assignments  $C$  and the Hawkes process parameters for all block pairs  $(\mu, \alpha, \beta)$ , each of which is a  $k \times k$  matrix. The vector of block assignment probabilities  $\pi$  can be easily estimated after estimating  $C$ . As with many other block models, the maximum-likelihood estimator (MLE) is intractable except for extremely small networks (e.g. 10 nodes) due to the discrete block assignments  $C$ . We propose an alternative estimation procedure in the following.

The estimation procedure for the proposed CHIP model has two components as shown in Algorithm 2: a community detection component and a parameter estimation component. For the community detection component, we employ a spectral clustering procedure on

a suitable *directed* adjacency matrix constructed from the event matrix  $Y$ . We define two notions of adjacency matrices. We define an unweighted directed adjacency matrix  $A$  where  $A_{ij}(T) = 1$  if there is at least one event from node  $i$  to node  $j$  up to time  $T$  and  $A_{ij}(T) = 0$  otherwise. We also define a weighted directed adjacency matrix  $N(T)$ , where  $N_{ij}(T)$  denotes the total number of events that have taken place from node  $i$  to node  $j$  by time  $T$ . Thus, we refer to  $N(T)$  also as the count matrix. For simplicity, we typically drop the dependence of  $T$  and refer to these adjacency matrices simply as  $A$  and  $N$ . An illustration of the two adjacency matrices constructed from an event matrix is shown in Figure 1. Junuthula et al. (2019) proposed to estimate the block assignments by applying spectral clustering to  $A$ . We consider both spectral clustering on the unweighted adjacency matrix  $A$  and the weighted adjacency matrix  $N$ . We will demonstrate in Section 4.1.4 that, in some cases, using  $A$  is superior to using  $N$  and vice-versa. After the community detection step, we can obtain an estimate  $\hat{C}$  of the block assignments, which we can use to estimate the block assignment probabilities

$$\hat{\pi}_a = \frac{1}{n} \sum_{i=1}^n \hat{C}_{ia}$$

for all  $a = 1, \dots, k$ .

For the parameter estimation component, we first consider estimating the Hawkes process parameters  $(\mu_{ab}, \alpha_{ab}, \beta_{ab})$  for each block pair  $(a, b)$  using only the weighted adjacency or count matrix  $N$ , i.e. without access to the event timestamps. Even without access to the event timestamps, we are able to estimate  $\mu_{ab}$  and the ratio  $m_{ab} = \alpha_{ab}/\beta_{ab}$ , but not the parameters  $\alpha_{ab}$  and  $\beta_{ab}$  separately. Define the following terms:

$$\bar{N}_{ab} = \frac{1}{n_{ab}} \sum_{i,j:C_{ia}=1,C_{jb}=1} N_{ij} \quad (2)$$

$$S_{ab}^2 = \frac{1}{n_{ab} - 1} \sum_{i,j:C_{ia}=1,C_{jb}=1} (N_{ij} - \bar{N}_{ab})^2, \quad (3)$$

where  $n_{ab}$  denotes the number of node pairs in block pair  $(a, b)$  and is given by

$$n_{ab} = \begin{cases} |a||b|, & a \neq b \\ |a||a-1|, & a = b \end{cases}$$

where  $|a|$  denotes the number of nodes in block  $a$ .  $\bar{N}_{ab}$  and  $S_{ab}^2$  are unbiased estimators of the mean and variance, respectively, of the counts of the number of events between all node pairs  $(i, j)$  in block pair  $(a, b)$ . We propose the following estimators for  $m_{ab}$  and  $\mu_{ab}$  from the count matrix  $N$ :

$$\hat{m}_{ab} = 1 - \sqrt{\frac{\bar{N}_{ab}}{S_{ab}^2}} \quad (4)$$

$$\hat{\mu}_{ab} = \frac{1}{T} \sqrt{\frac{(\bar{N}_{ab})^3}{S_{ab}^2}}. \quad (5)$$

We note that, in some prior work, exponential Hawkes processes are parameterized only in terms of  $m$  and  $\mu$ , with  $\beta$  treated as a known parameter that is not estimated (Bacry



et al., 2016, 2017). In this case, the estimation procedure is complete. On the other hand, if we want to estimate the values of both  $\alpha$  and  $\beta$  rather than just their ratio, we have to use the actual event matrix  $Y$  with the event timestamps. To separately estimate the  $\alpha_{ab}$  and  $\beta_{ab}$  parameters, we replace  $\alpha_{ab} = \beta_{ab}m_{ab}$  in the exponential Hawkes log-likelihood (1) for block pair  $(a, b)$  to obtain

$$\begin{aligned} & \log \mathcal{L}(\beta_{ab}|C, [\mathbf{t}_{ij}]_{i,j=1}^n) \\ = & \sum_{i,j:C_{ia}=1,C_{jb}=1} \left\{ -\mu_{ab}T + \sum_{q=1}^{N_{ij}} m_{ab} \{e^{-\beta_{ab}(T-t_{ij}^q)} - 1\} + \sum_{q=1}^{N_{ij}} \log(\mu_{ab} + \beta_{ab}m_{ab}w_{ij}(q)) \right\} \quad (6) \end{aligned}$$

where  $w_{ij}(q) = \sum_{q':t_{ij}^{q'} < t_{ij}^q} e^{-\beta_{ab}(t_{ij}^q - t_{ij}^{q'})}$  for  $q \geq 2$  and  $w_{ij}(1) = 0$ . We substitute in the estimates for  $m_{ab}$  and  $\mu_{ab}$  from (4) and (5), respectively. Then the log-likelihood (6) is purely a function of  $\beta_{ab}$  and can be maximized using a standard scalar optimization or line search method.

## 4. Theoretical Analysis of Estimators

We first derive non-asymptotic upper bounds on the misclustering error in the estimated community memberships both in the general setting and in a simplified setting typically employed in the literature. We then derive consistency and asymptotic normality properties of the estimators for the Hawkes process parameters.

### 4.1 Analysis of Estimated Community Assignments

We derive upper bounds on the error rate of community detection using spectral clustering on both the unweighted and the weighted adjacency matrices. We denote the true vector of community assignments and the vector of community assignments obtained from a method as  $\mathbf{c}$  and  $\hat{\mathbf{c}}$  respectively. Then the error of community detection can be defined as the fraction of nodes whose community is wrongly attributed to a community other than its true community, i.e.,  $r = \inf_{\Pi} \frac{1}{n} \sum_{i=1}^n 1(\mathbf{c}_i \neq \Pi(\hat{\mathbf{c}}_i))$ , where  $\Pi(\cdot)$  denotes the set of all permutations of the community labels.

While our proposed CHIP model considers directed events, which lead to directed adjacency matrices, our analysis in this section considers undirected adjacency matrices to better match up with the majority of the literature on analysis of spectral clustering for the SBM. For undirected adjacency matrices, spectral clustering is performed by running k-means clustering on the rows of the *eigenvector* matrix, not the rows of the concatenated singular vector matrix as shown in Section 2.2. The bounds and consistency properties we derive still apply to the directed case with only a change in the constant.

#### 4.1.1 ESTIMATED COMMUNITIES FROM UNWEIGHTED ADJACENCY MATRIX

We form the binary adjacency matrix  $A$  from the observed counts as  $A_{ij} = 1\{N_{ij} > 0\}$ , i.e., there is a 1 at the  $(i, j)$ th position if there is at least one event between nodes  $i$  and  $j$ . Then for a pair of nodes  $(i, j)$  such that  $c_i = a$  and  $c_j = b$ , we have

$$E[A_{ij}] = E[1\{N_{ij} > 0\}] = P(N_{ij} > 0) = 1 - P(N_{ij} = 0) = 1 - \exp(-\mu_{ab}T),$$

where the last step follows since we assume the processes are at the baseline intensities governed by the parameters  $\mu$  at the starting point of our observation period. In the absence of any event, the intensity does not jump and remains at the level  $\mu_{ab}$  which then boils down to a homogeneous Poisson process.

An important step in understanding whether the algorithms will succeed in estimating the community assignments consistently is to determine whether the algorithms can obtain the true community assignments correctly (i.e., without any error) if there were no sampling error and we were given the population (expected) versions of the unweighted adjacency and the weighted count matrices respectively. We note that  $E[A] = C(1 - \exp(\mu T))C^T$ , i.e.  $E[A]$  takes the form of a stochastic block model with the matrix of block parameters given by  $(1 - \exp(\mu T))$ . We assume that  $\mu$  is non-singular, i.e. of full rank. Then by Lemma 3.1 of Rohe et al. (2011), the top  $k$  eigenvectors (and those corresponding to non-zero eigenvalues) of the matrix  $E[A]$  are given by  $Cu$  where  $u$  is an invertible matrix. Since  $u$  is an invertible matrix,  $C_i u = C_j u$  for some  $(i, j)$  implies that  $C_i = C_j$  up to the ambiguity of label permutations. Hence running an  $(1 + \epsilon)$ -approximate k-means algorithm (Kumar et al., 2004; Lei and Rinaldo, 2015) will correctly identify the communities from this matrix.

Now  $A$  is a  $n \times n$  symmetric matrix whose elements  $A_{ij}$  are independent Bernoulli random variables with mean  $E[A_{ij}]$ . Let  $\Delta = \max\{n \max_{i,j} E[A_{ij}], c_0 \log n\}$  for some constant  $c_0$ , and note that  $n \max_{i,j} E[A_{ij}] = n \max(1 - \exp(-\mu_{ab} T)) = n(1 - \exp(-\mu_{\max} T))$ , where  $\mu_{\max} = \max_{a,b} \mu_{ab}$ . Further, let  $\lambda_{\min}(E[A])$  denote the minimum in absolute value non-zero eigenvalue of the matrix  $E[A]$  and  $|a|_{\max}$  denote the size of the largest community. Then we have the following upper bound on the error rate of spectral clustering performed on  $A$ .

**Theorem 1** *Let  $Y$  be a relational event matrix on  $n$  nodes generated according to a  $k$ -block CHIP model with community assignment matrix  $C$  and parameter matrices  $\mu, \alpha, \beta$ . Let  $A$  be the binary adjacency matrix obtained from  $Y$  at time  $T$ . Then with probability at least  $1 - n^{-r}$ , the misclustering error rate of community detection by applying spectral clustering to the matrix  $A$  is,*

$$r_A \leq 64(2 + \epsilon) \frac{|a|_{\max} k c \Delta}{n(\lambda_{\min}(E[A]))^2}, \quad (7)$$

where  $\epsilon > 0$  is a constant and  $c > 0$  is a constant dependent on  $c_0$  and  $r$ .

The proof of this theorem and all other subsequent theorems on estimated community assignments can be found in Appendix A.1.

#### 4.1.2 ESTIMATED COMMUNITIES FROM WEIGHTED ADJACENCY (COUNT) MATRIX

Next we investigate the error in recovering the community structure by applying spectral clustering algorithm to the weighted aggregate adjacency matrix  $N$ . Throughout this section we make an additional assumption of  $T \rightarrow \infty$ , i.e. the system is observed for a long time. Under the CHIP model, the expectation and variance of the number of events between nodes  $(i, j)$  is (Hawkes and Oakes, 1974; Hawkes, 1971a; Lewis, 1969)

$$\nu_{ab} = E[N_{ij} | C_{ia} = 1, C_{jb} = 1] = \frac{\mu_{ab} T}{1 - \alpha_{ab}/\beta_{ab}} \quad (8)$$

$$\sigma_{ab}^2 = V[N_{ij} | C_{ia} = 1, C_{jb} = 1] = \frac{\mu_{ab} T}{(1 - \alpha_{ab}/\beta_{ab})^3}. \quad (9)$$

Similar to the unweighted case, we first show that the algorithm can obtain the true community assignments correctly (i.e. without any error) if there were no sampling error and we were given the population count matrix  $E[N]$ . We note that  $E[N] = C\nu C^T$ , where  $\nu$  is a  $k \times k$  symmetric matrix whose elements are given by  $\nu_{ab}$ , as defined in (8). We again assume that  $\nu$  is non-singular, i.e. of full rank. Then using the same arguments as before, we conclude that the spectral algorithm applied to  $E[N]$  will correctly recover the community assignments.

However we do not observe the population aggregate matrix  $E[N]$ , but instead its “noisy” realization (sample)  $N$ . To characterize the misclustering rate of a spectral clustering algorithm applied to  $N$ , we define the following quantities. Let  $\lambda_{\min}(E[N])$  denote the minimum in absolute value non-zero eigenvalue of the matrix  $E[N]$ . Define

$$\begin{aligned} s &= \max_i \sqrt{\sum_j V[N_{ij} | C_{ia} = 1, C_{jb} = 1]} \\ &= \sqrt{T} \max_i \sqrt{\sum_j \frac{\mu_{ab}}{(1 - \alpha_{ab}/\beta_{ab})^3}} \\ &= \sqrt{T} \max_a \sqrt{\sum_b |b| \frac{\mu_{ab}}{(1 - \alpha_{ab}/\beta_{ab})^3}} \end{aligned} \quad (10)$$

and

$$s_1 = \max_{i,j} \sqrt{V[N_{ij} | C_{ia} = 1, C_{jb} = 1]} = \sqrt{T} \max_{a,b} \sqrt{\frac{\mu_{ab}}{(1 - \alpha_{ab}/\beta_{ab})^3}}. \quad (11)$$

Then we have the following upper bound on the misclustering error rate.

**Theorem 2** *Let  $Y$  be a relational event matrix on  $n$  nodes generated according to a  $k$ -block CHIP model with community assignment matrix  $C$  and parameter matrices  $\mu, \alpha, \beta$ . Let  $N$  be the weighted adjacency matrix obtained by aggregating  $Y$  at time  $T$ . Then with probability at least  $1 - 1/n$ , the misclustering error rate of community detection by applying spectral clustering to the matrix  $N$  is,*

$$r_N \leq 64(2 + \epsilon_1) \frac{|a|_{\max} k \left\{ (1 + \epsilon)(2s + \frac{6}{\log(1+\epsilon)} s_1 \sqrt{\log n}) + s_1 \sqrt{\log n} \right\}^2}{n(\lambda_{\min}(E[N]))^2}, \quad (12)$$

where  $0 < \epsilon < 1/2$  and  $\epsilon_1 > 0$  are constants.

**Remark** Note that the assumption of  $T \rightarrow \infty$  does not preclude us from being able to analyze scenarios where the communications are sparse since the expected number of communications between a pair of nodes  $\nu_{ab}$  can be made constant or even  $o(1)$  by setting  $\frac{\mu_{ab}}{1 - \alpha_{ab}/\beta_{ab}} = O(1/T)$  and  $\frac{\mu_{ab}}{1 - \alpha_{ab}/\beta_{ab}} = o(1/T)$  respectively.

It is also possible to obtain an expression for the mean as a function of  $T$  without the assumption of  $T \rightarrow \infty$  using stochastic differential equations (Laub et al., 2015; Da Fonseca and Zaatour, 2014). In particular, if we substitute the starting intensity  $\lambda_0 = \mu$ , i.e., the process starts with baseline intensity as we have assumed throughout, and the starting

number of events  $N_0 = 0$ , then from the result of Da Fonseca and Zaatour (2014) and Daw and Pender (2018),

$$E[N_{ij}] = \frac{\mu_{ab}T}{1 - \alpha_{ab}/\beta_{ab}} - \mu_{ab} \left( \frac{\alpha_{ab}}{\beta_{ab} - \alpha_{ab}} \right) \left( \frac{1 - e^{-(\beta_{ab} - \alpha_{ab})T}}{\beta_{ab} - \alpha_{ab}} \right)$$

We note that there is a small negative correction term to the asymptotic mean, whose effect is negligible as  $T \rightarrow \infty$ .

#### 4.1.3 SIMPLIFIED SPECIAL CASES

The upper bounds on the error rate in Theorems 1 and 2 are not very informative in terms of their dependencies on key model parameters. To understand such dependence better, we consider some simplified special cases of our CHIP model which are in similar spirit as commonly employed in the stochastic block model literature (Rohe et al., 2011; Lei and Rinaldo, 2015; Paul and Chen, 2017; Chin et al., 2015; Gao et al., 2017).

**Case 1:  $k$  equivalent communities** We first consider the following simplified special case: all communities have equal number of elements  $|a| = \frac{n}{k}$ , all intra-community processes (diagonal block pairs) have the same set of parameters  $\mu_1, \alpha_1, \beta_1$  and all inter-community processes (off-diagonal block pairs) have the same set of parameters  $\mu_2, \alpha_2, \beta_2$ . We use the notation  $Y \sim \text{CHIP}(C, n, k, \mu_1, \alpha_1, \beta_1, \mu_2, \alpha_2, \beta_2)$  to denote a relational event matrix  $Y$  generated from this simplified model. Define  $m_1 = \frac{\alpha_1}{\beta_1}$  and  $m_2 = \frac{\alpha_2}{\beta_2}$ . Let  $\nu_1 = \frac{\mu_1}{(1-m_1)}$  and  $\nu_2 = \frac{\mu_2}{(1-m_2)}$ , while  $\sigma_1^2 = \frac{\mu_1}{(1-m_1)^3}$  and  $\sigma_2^2 = \frac{\mu_2}{(1-m_2)^3}$ . Assume  $\nu_1 > \nu_2$ ,  $\nu_1 \asymp \nu_2$ , and  $\sigma_1 \asymp \sigma_2$ , where the asymptotic equivalence is with respect to both  $n$  and  $T$ . These assumptions imply that the expected number of events are higher between two nodes in the same community compared to two nodes in different communities and that the asymptotic dependence on  $n$  and  $T$  are same for both set of parameters. This setting is useful to understand detectability limits and has been widely employed in the literature on stochastic block models (Abbe and Sandon, 2015; Gao et al., 2017; Chin et al., 2015; Vu, 2018; Abbe, 2017; Paul and Chen, 2017). We have a number of corollaries to the two theorems under this model.

First, we have the following result for spectral clustering using the unweighted adjacency matrix  $A$ .

**Corollary 1** *Let  $Y \sim \text{CHIP}(C, n, k, \mu_1, \alpha_1, \beta_1, \mu_2, \alpha_2, \beta_2)$ . The misclustering rate of community detection by applying spectral clustering on the binary adjacency matrix  $A$  obtained from  $Y$  at time  $T$  is*

$$r_1 \lesssim \frac{n(1 - \exp(-\mu_1 T))}{(n/k)^2(\exp(-\mu_2 T) - \exp(-\mu_1 T))^2} \asymp \frac{k^2}{n} \frac{1 - \exp(-\mu_1 T)}{(\exp(-\mu_2 T) - \exp(-\mu_1 T))^2}. \quad (13)$$

If further we assume  $\mu_1 \asymp \mu_2 \asymp o(1/T)$ , such that  $\mu_1 T = o(1)$  and  $\mu_2 T = o(1)$ , then we have

$$r_1 \lesssim \frac{nT\mu_1}{(n/k)^2(\mu_1 - \mu_2)^2 T^2} \asymp \frac{k^2}{nT} \frac{\mu_1}{(\mu_1 - \mu_2)^2}, \quad (14)$$

whereas, for  $\mu_1 \asymp \mu_2 \asymp \omega(1/T)$ , such that  $\mu_1 T \rightarrow \infty$  and  $\mu_2 T \rightarrow \infty$ , then the upper bound for the misclustering rate in Theorem 1 goes to 1.

We note that if the parameters are kept constant as a function of  $T$ , then  $\mu_1 T \rightarrow \infty$  and  $\mu_2 T \rightarrow \infty$ . Consequently, without  $k$  and  $n$  changing the upper bound on the error rate for the unweighted adjacency matrix in Theorem 1 explodes and becomes close to 1, making the upper bound guarantee useless. While this result might be a drawback of the upper bound result itself, we note that unbounded error makes sense because in this regime almost all node pairs have at least one communication with high probability. Hence the unweighted adjacency matrix has 1 in almost all entries and the community structure cannot be detected from this matrix. In that case, we predict that using the weighted adjacency matrix can lead to smaller error. In the absence of matching lower bounds, we will experimentally test this assertion in a simulation in Section 5.1.2.

Next we have the following corollary for spectral clustering using the weighted count matrix  $N$ .

**Corollary 2** *Let  $Y \sim \text{CHIP}(C, n, k, \mu_1, \alpha_1, \beta_1, \mu_2, \alpha_2, \beta_2)$ . The misclustering rate of community detection by applying spectral clustering on the weighted adjacency matrix  $N$  aggregated from  $Y$  at time  $T$  is*

$$r \lesssim \frac{T\sigma_1^2 n}{(n/k)^2(\nu_2 - \nu_1)^2 T^2} \asymp \frac{k^2}{nT} \frac{\sigma_1^2}{(\nu_1 - \nu_2)^2}.$$

We note that if the set of parameters  $\mu, \alpha, \beta$  remain constant as a function of  $n$  and  $T$  then the misclustering error rate decreases as  $1/T$  with increasing  $T$ , decreases as  $1/n$  with increasing  $n$ , and increases as  $k$  with increasing  $k$ . Hence, as we observe the process for more time, spectral clustering on the aggregate matrix has lower error rate. The rate of convergence with increasing  $T$  is the same as one would obtain for detecting an average community structure if discrete snapshots of the network was available over time (Pensky et al., 2019; Paul and Chen, 2017; Bhattacharyya and Chatterjee, 2018). The dependence of the misclustering error rate on  $n$  and  $k$  is what one would expect from the SBM literature.

However, the density of the aggregate adjacency matrix is governed by the parameters of the CHIP model. Hence, to further characterize the dependence of the  $\mu$  parameters on the number of nodes  $n$  and time  $T$  in the network, assume  $\mu_1 = c_1 \frac{1}{f(n)g(T)}$  and  $\mu_2 = c_2 \frac{1}{f(n)g(T)}$ , where  $c_1$  and  $c_2$  are constants that do not depend on  $n$  or  $T$ . Also assume  $1 - \alpha_1/\beta_1$  and  $1 - \alpha_2/\beta_2$  do not depend on  $n$  and  $T$ . Then the upper bound on the error rate becomes

$$r \lesssim \frac{k^2 f(n)g(T)}{nT(c_1 - c_2)^2}.$$

Now we note that consistent community detection is possible as long as  $k = o\left(\frac{\sqrt{nT}|c_1 - c_2|}{f(n)g(T)}\right)$ . For example, if we set  $g(T) \asymp T$  and  $f(n) = \frac{n}{\log n}$ , such that  $\mu_1 \asymp \mu_2 \asymp \frac{\log n}{nT}$ , then the expected number of events between a node pair is  $O\left(\frac{\log n}{n}\right)$  and total expected number of events in the whole network is  $O(n \log n)$ . In that case,  $r(T) \lesssim \frac{k^2}{\log n (c_1 - c_2)^2}$ , and consistent community detection is possible as long as  $k = o(\sqrt{\log n} |c_1 - c_2|)$ .

A second example is where we set  $g(T) \asymp 1$  and  $f(n) = \frac{n}{\log n}$ , such that  $\mu_1 \asymp \mu_2 \asymp \frac{\log n}{n}$ . The expected number of events between a vertex pair is then  $O\left(\frac{T \log n}{n}\right)$  and total expected

number of events in the whole network is  $O(nT \log n)$ . In that case  $r \lesssim \frac{k^2}{T \log n (c_1 - c_2)^2}$ , and consistent community detection is possible as long as  $k = o(\sqrt{T \log n} |c_1 - c_2|)$ .

**Case 2: Two equivalent communities** Another special set-up that is widely analyzed in the SBM literature on detectability limits is a special case of the previous set-up where we have  $2n$  nodes equally divided between  $k = 2$  communities (Abbe, 2017). We have the following two corollaries for the unweighted and weighted adjacency matrices under this model.

**Corollary 3** *Let  $Y \sim \text{CHIP}(C, 2n, 2, \mu_1, \alpha_1, \beta_1, \mu_2, \alpha_2, \beta_2)$ . The misclustering rate of community detection by applying spectral clustering on the binary adjacency matrix  $A$  obtained from  $Y$  at time  $T$  is*

$$r_1 \lesssim \frac{1}{n} \frac{1 - \exp(-\mu_1 T)}{(\exp(-\mu_2 T) - \exp(-\mu_1 T))^2}.$$

If further we assume  $\mu_1 \asymp \mu_2 \asymp o(1/T)$ , such that  $\mu_1 T = o(1)$  and  $\mu_2 T = o(1)$ , then we have

$$r_1 \lesssim \frac{1}{nT} \frac{\mu_1}{(\mu_1 - \mu_2)^2}.$$

**Corollary 4** *Let  $Y \sim \text{CHIP}(C, 2n, 2, \mu_1, \alpha_1, \beta_1, \mu_2, \alpha_2, \beta_2)$ . The misclustering rate of community detection by applying spectral clustering on the weighted adjacency matrix  $N$  obtained from  $Y$  at time  $T$  is*

$$r \lesssim \frac{nT(\sigma_1^2 + \sigma_2^2)}{n^2(\nu_1 - \nu_2)^2 T^2} \asymp \frac{1}{nT} \frac{(\sigma_1^2 + \sigma_2^2)}{(\nu_1 - \nu_2)^2}.$$

Detection limits can be obtained in this case similar to the  $k$ -community case. We use these results to compare error rates between the unweighted and weighted adjacency matrix variants in the following.

#### 4.1.4 COMPARISON BETWEEN WEIGHTED AND UNWEIGHTED ADJACENCY MATRICES

We compare the bounds on the error rates in weighted and unweighted adjacency matrices in corollaries 3 and 4 in the sparse regime where  $\mu_1 T$  and  $\mu_2 T$  are small such that we can apply the Taylor series approximation. From Corollary 3, we have the error rate using the unweighted adjacency matrix is upper bounded by  $\frac{1}{nT} \frac{\mu_1}{(\mu_1 - \mu_2)^2}$ , while the error rate for the weighted adjacency matrix is upper bounded by

$$\frac{1}{nT} \frac{\frac{\mu_1}{(1-m_1)^3} + \frac{\mu_2}{(1-m_2)^3}}{\left(\frac{\mu_1}{(1-m_1)} - \frac{\mu_2}{(1-m_2)}\right)^2}$$

from Corollary 4. We can make the following comparison comments on the basis of these upper bounds. In the absence of matching lower bounds, we will verify these through simulations in Sections 5.1.1 and 5.1.2.

1. If  $m_1 = m_2 = m$  such that the community structure is expressed only through  $\mu_1$  and  $\mu_2$ , then the error for the weighted adjacency matrix is bounded by  $\frac{1}{nT} \frac{\mu_1 + \mu_2}{(\mu_1 - \mu_2)^2} \frac{1}{1-m}$ . We note that this upper bound is higher than the corresponding upper bound for spectral clustering in unweighted adjacency matrix indicating a possible advantage of using the unweighted adjacency matrix.
2. If  $\mu_1 = \mu_2$  such that the community structure is expressed purely through  $\alpha, \beta$ , then clearly the error for unweighted case is unbounded. However, the error for the weighted case can still be bounded indicating a possible advantage of using the weighted adjacency matrix.

#### 4.2 Analysis of Estimated Hawkes Process Parameters

As discussed in Section 3.2, we are able to estimate  $m = \alpha/\beta$  and  $\mu$  from the count matrix  $N$  using (4) and (5), respectively. We analyze these estimators assuming a growing number of nodes  $n$  and time duration  $T$ . We do not put any assumption on the distribution of the counts; we only require that  $T$  is large enough such that the asymptotic (stationary) mean and variance holds for the counts, i.e.  $E[N_{ij}] = \nu_{ab}$  and  $V[N_{ij}] = \sigma_{ab}^2$  for node pair  $(i, j)$  that belongs to block pair  $(a, b)$ . From their definitions in (2) and (3), it is easy to see that  $\bar{N}_{ab}$  and  $S_{ab}^2$  are unbiased estimators of  $\nu_{ab}$  and  $\sigma_{ab}^2$ , respectively. The following theorem shows that these estimators are consistent and asymptotically normal using a combination of the Central Limit Theorem, the delta method and Slutsky's lemma.

**Theorem 3** *Define  $n_{\min} = \min_{a,b} n_{ab}$ . The estimators for  $m_{ab}$  and  $\mu_{ab}$  have the following asymptotic distributions as  $n_{\min} \rightarrow \infty$  and  $T \rightarrow \infty$ :*

$$\begin{aligned} \sqrt{n_{ab}} \left( \hat{m}_{ab} - \left( 1 - \sqrt{\frac{\nu_{ab}}{\sigma_{ab}^2}} \right) \right) &\xrightarrow{d} \mathcal{N} \left( 0, \frac{1}{4\nu_{ab}} \right) \\ \sqrt{n_{ab}} \left( \hat{\mu}_{ab} T - \frac{(\nu_{ab})^{3/2}}{\sigma_{ab}} \right) &\xrightarrow{d} \mathcal{N} \left( 0, \frac{9}{4} \nu_{ab} \right). \end{aligned}$$

The proof is provided in Appendix A.2. Note that, in the simplified special case of equal community sizes mentioned in Section 4.1.3, we have  $n_{ab} \asymp (\frac{n}{k})^2$ . Therefore, the condition  $n_{\min} \rightarrow \infty$  boils down to  $\frac{n^2}{k^2} \rightarrow \infty$ . Further, the rate of convergence for both  $\hat{m}_{ab}$  and  $\hat{\mu}_{ab} T$  to their respective expected values in Theorem 3 is  $O(\frac{n}{k})$ . This implies that the mean squared error (MSE) of both the parameters decreases as  $O(\frac{n^2}{k^2})$  as  $n$  increases. In particular, if  $k$  remains constant as  $n$  increases, we expect the MSE of the two parameters to decrease at a quadratic rate.

## 5. Experiments

We begin with a set of simulation experiments to assess the accuracy of our proposed estimation procedure and verify our theoretical analysis. We then present several experiments on real data involving both prediction and model-based exploratory analysis. Code to replicate our experiments is available at <https://github.com/IdeasLabUT/CHIP-Network-Model>.

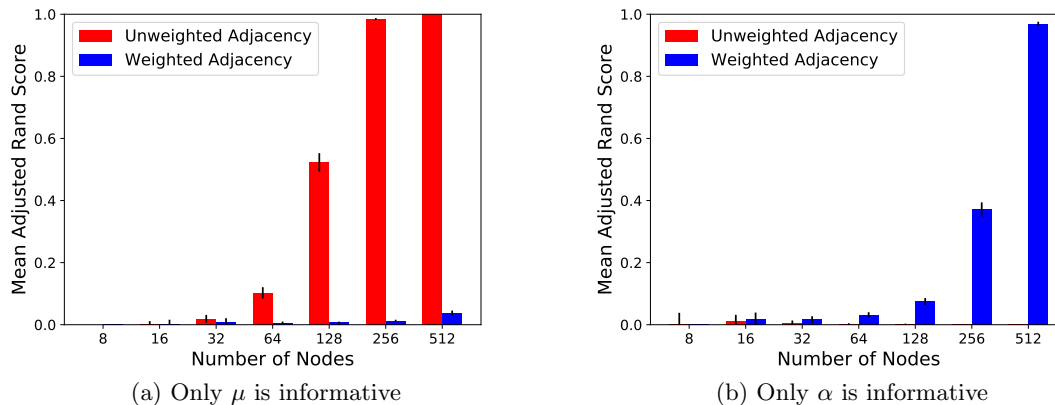


Figure 2: Mean adjusted Rand score of spectral clustering on weighted and unweighted adjacency matrices over 100 simulated networks ( $\pm 2$  standard errors). (a)  $\mu_1 \neq \mu_2$  and  $\alpha_1 = \alpha_2$ . (b)  $\mu_1 = \mu_2$  and  $\alpha_1 \neq \alpha_2$ .  $\beta_1 = \beta_2$  in both cases.

## 5.1 Simulated Networks

This section will include four separate experiments. The first three are designed to analyze the effects of various parameters of the CHIP model on the accuracy of spectral clustering, and to compare spectral clustering using weighted and unweighted adjacency matrices in detecting the ground truth community structure in simulated networks. The fourth experiment is focused on the consistency of estimating the CHIP Hawkes process parameters.

### 5.1.1 SPECTRAL CLUSTERING ON WEIGHTED VS. UNWEIGHTED ADJACENCY MATRIX

Our first experiment compares spectral clustering using the weighted adjacency (count) matrix  $N$  and unweighted adjacency matrix  $A$  in terms of accuracy of community detection on simulated networks. We simulate networks from the simplified CHIP model described in Section 4.1.3 with  $k = 4$  communities, duration  $T = 400$ , and a growing number of nodes  $n$ . Since the estimated community labels will be permuted compared to the actual community labels, we evaluate the community detection accuracy using the adjusted Rand score (Hubert and Arabie, 1985), which is 1 for perfect community detection and has an expectation of 0 for a random community detection.

First, we choose parameters  $\mu_1 = 0.002$ ,  $\mu_2 = 0.001$ ,  $\alpha_1 = \alpha_2 = 7$ , and  $\beta_1 = \beta_2 = 8$ . In this setting, only  $\mu$  is informative, and the upper bound on the misclustering error rate using the weighted adjacency matrix is expected to be worse by a factor of  $(1 - m)^{-1} = 8$  as discussed in Section 4.1.4. The adjusted Rand scores for spectral clustering on both the weighted and unweighted adjacency matrices over 100 simulated networks for each value of  $n$  are shown in Figure 2a. Notice that the accuracy on the unweighted adjacency matrix approaches 1 for growing  $n$ , as expected. On the other hand, the accuracy on the weighted adjacency matrix is significantly worse and no better than a random community assignment until  $n = 512$  nodes. Thus, we see that the actual community detection accuracy for the



weighted adjacency matrix is significantly worse than on the unweighted adjacency matrix, as predicted by the comparison of the respective upper bounds on the misclustering error rates.

Next, we choose parameters  $\mu_1 = \mu_2 = 0.001$ ,  $\alpha_1 = 0.006$ ,  $\alpha_2 = 0.001$ , and  $\beta_1 = \beta_2 = 0.008$ . In this setting, only  $\alpha$  is informative, so the error for the unweighted adjacency matrix is unbounded, while the error for the weighted adjacency matrix still follows the upper bound in Corollary 2. Therefore, as we observe in Figure 2b, the accuracy on the weighted adjacency matrix approaches 1 as  $n$  increases, while the accuracy on the unweighted adjacency is no better than random even for growing  $n$ .

### 5.1.2 EFFECTS OF DIAGONAL AND OFF-DIAGONAL $\mu$ 'S ON COMMUNITY DETECTION

In Section 5.1.1 we observed that community detection will be easier if  $\mu$  is informative ( $\mu_1 \neq \mu_2$ ). In this experiment, we will explore two different ways of encoding community information into simulated networks by

1. Scaling up both  $\mu_1$  and  $\mu_2$ , while keeping a fixed  $\mu_1 : \mu_2$  ratio.
2. Only scaling up  $\mu_1$ , allowing for  $\mu_1 : \mu_2$  ratio to increase.

Both settings share the same base parameters of  $\mu_1 = 0.075$  and  $\mu_2 = 0.065$ , with  $k = 4$  communities and  $n = 128$  nodes, a duration of  $T = 50$ , where  $\alpha_1 = \alpha_2 = 0.05$  and  $\beta_1 = \beta_2 = 0.08$ . These parameters are chosen to create a base network that is nearly impossible for spectral clustering to accurately detect communities. The objective is similar to that of Section 5.1.1, where in both settings we perform community detection using spectral clustering on the weighted adjacency of simulated networks, while increasing  $\mu_1$  and  $\mu_2$  or their ratio. Lastly, we average over the adjusted Rand score of 100 simulations.

As shown in Figure 3, community detection accuracy increases in both settings as the scalars increase; however, we find that the increase in accuracy occurs for different reasons. In the first setting, Figure 3a, where both  $\mu$ 's are scaled up with a fixed ratio, community detection becomes easier simply because the networks are becoming denser, as shown in the numbers above the bars in Figure 4, and more information is available. Furthermore, although we keep the  $\mu_1 : \mu_2$  ratio fixed, as the scalars increase the difference between the two starts to magnify. On the other hand, as networks become denser and most node pairs start to have at least one interaction, it is only the number of interactions among node pairs that becomes informative. Therefore, spectral clustering on the weighted adjacency matrix continues to result in a high adjusted Rand score, while the adjusted Rand score of spectral clustering on the unweighted adjacency matrix decreases with increasing density, as it is illustrated in Figure 4. This observation confirms the theoretical prediction made in Corollary 1. The opposite also holds to some degree. For really sparse networks spectral clustering is more accurate on the unweighted adjacency matrix; however, in Figure 4 we observe that it loses its advantage as the proportion of node pairs with at least one interaction approaches 0.5 and starts impairing community detection as it passed 0.8.

In the second setting, Figure 3b, by only scaling up  $\mu_1$ , the difference between the baseline rate of occurrence of an event between the diagonal and the off-diagonal blocks increases. This increases the signal-to-noise ratio and is a more effective way of encoding community information into a network. This can be observed by comparing the scalars of

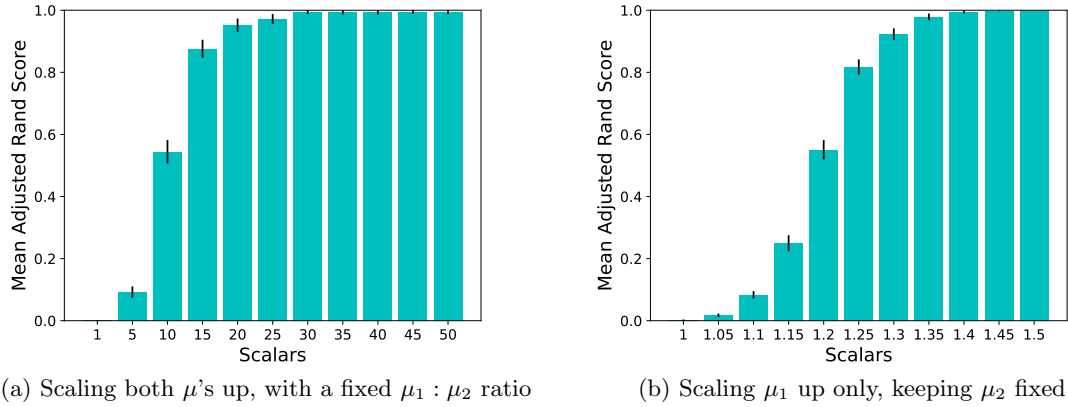


Figure 3: Adjusted Rand score of spectral clustering on weighted adjacency matrix, averaged over 100 simulated networks ( $\pm 2$  standard errors), while multiplying  $\mu_1$  and  $\mu_2$  or their ratio by scalars. (a) Scaling up both  $\mu_1$  and  $\mu_2$ , keeping their ratio fixed. (b) Only scaling up  $\mu_1$ , while keeping  $\mu_2$  fixed.

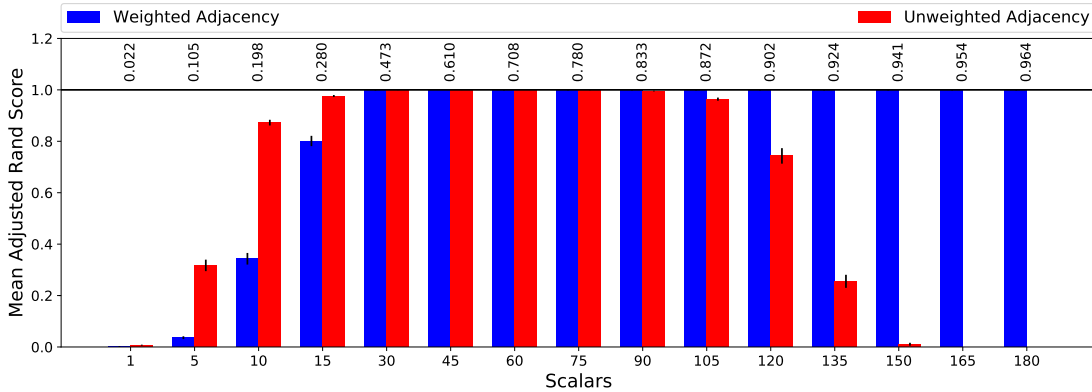


Figure 4: Adjusted Rand score of spectral clustering on weighted vs. unweighted adjacency matrices, averaged over 100 simulations ( $\pm 2$  standard errors), while multiplying both  $\mu_1$  and  $\mu_2$  by scalars. The numbers above each bar indicate the average density of simulated networks as the proportion of non-zero entries to the total number of elements in the adjacency matrix. Base model parameters are:  $\mu_1 = 7.5 \times 10^{-4}$ ,  $\mu_2 = 3.5 \times 10^{-4}$ ,  $k = 4$ ,  $T = 50$ ,  $n = 256$ ,  $\alpha_1 = \alpha_2 = 0.05$ , and  $\beta_1 = \beta_2 = 0.08$ .

Figures 3a and 3b. Starting from the same base network, a perfect adjusted Rand score is achieved when only  $\mu_1$  is scaled up by a factor of 1.4, compared to scaling both  $\mu$ 's up by a factor of 30.

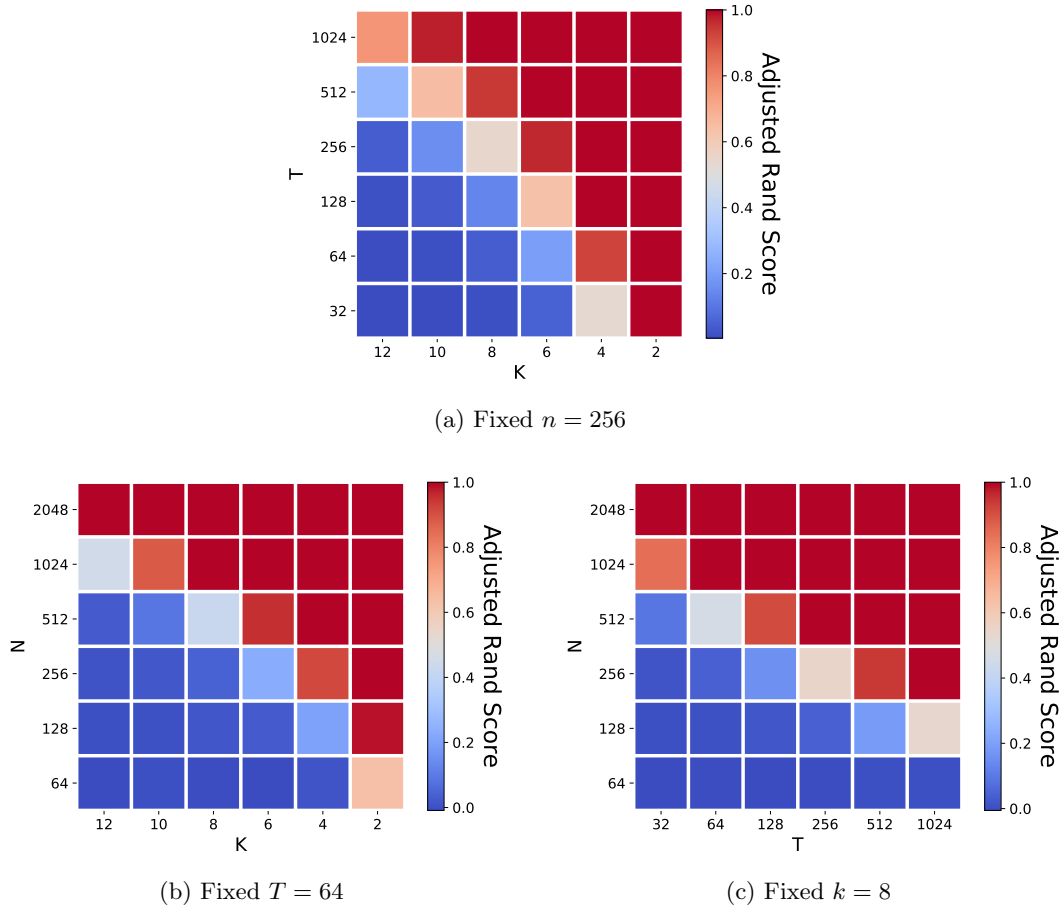


Figure 5: Heat map of adjusted Rand score of spectral clustering on weighted adjacency matrix, with varying  $T$ ,  $n$ , and  $k$ , averaged over 30 simulated networks.

### 5.1.3 COMMUNITY DETECTION WITH VARYING $T$ , $n$ , AND $k$

Here we will be analyzing the effects of the duration of the data trace  $T$ , its number of nodes  $n$ , and its number of communities  $k$ , on community detection using spectral clustering. Similar to our previous simulations, we will start by simulating a base network with the following parameters:  $T = 64$ ,  $n = 256$ ,  $k = 8$ ,  $\mu_1 = 0.085$ ,  $\mu_2 = 0.065$ ,  $\alpha_1 = \alpha_2 = 0.06$ , and  $\beta_1 = \beta_2 = 0.08$ . The upper bounds on the error rates in Section 4.1.3 involves all three parameters  $n, k, T$  simultaneously, making it difficult to interpret the result. To better observe the effects of  $T$ ,  $n$ , and  $k$  and their relationship with respect to each other, we perform three separate simulations each time varying two and fixing the other one to its default value. Similar to our previous experiments, for all simulated networks the objective is to measure the mean adjusted Rand score of spectral clustering on weighted adjacency matrix, averaged over 30 simulations.

In Figure 5, we observe the tradeoff and interplay among the model parameters as they are varied two at a time. Note that Corollary 2 predicts that the misclustering error rate

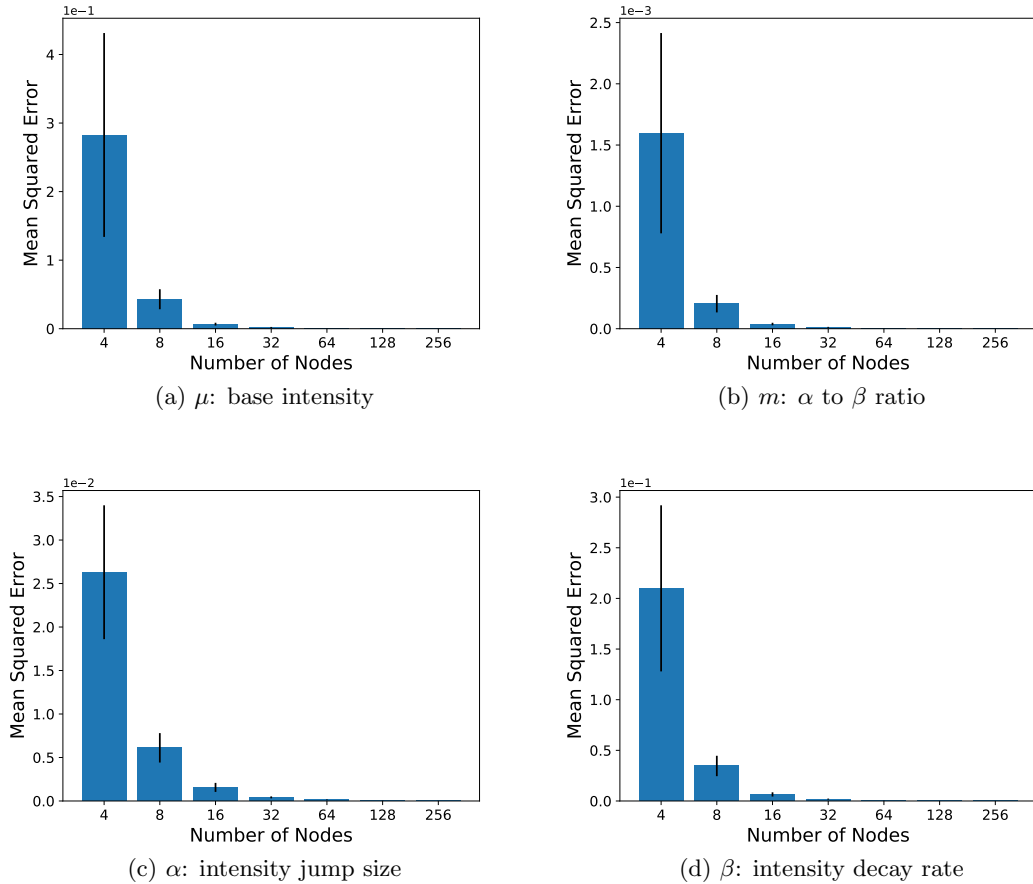


Figure 6: Mean-squared errors of CHIP’s Hawkes parameter estimators averaged over 100 simulations ( $\pm 2$  standard errors). We observe that MSE approaches zero as the number of nodes increases in a network which illustrates the consistency of these parameters as proven in Section 4.2.

varies as  $\frac{k^2}{nT}$  if all three parameters are varied. Figure 5a shows the accuracy to be low for small  $T$  and large  $k$ . As we simultaneously increase  $T$  and decrease  $k$  the accuracy improves until the adjusted Rand index reaches 1. We also note that it is possible to obtain high accuracy either with increasing  $T$  or decreasing  $k$  or with both even when  $n$  is fixed. This is in line with the prediction from Corollary 2 that the misclustering error rate varies as  $\frac{k^2}{T}$  if  $n$  remains fixed. We observe a similar effect of increasing accuracy with increasing  $n$  and decreasing  $k$  when  $T$  is kept fixed in Figure 5b. Finally, Figure 5c verifies the prediction that accuracy increases with both increasing  $n$  and  $T$  for a fixed  $k$ .

#### 5.1.4 HAWKES PROCESS PARAMETER ESTIMATION

In this experiment, we verify the consistency of the  $\hat{m}$ ,  $\hat{\mu}$ ,  $\hat{\alpha}$ , and  $\hat{\beta}$  estimators of the Hawkes process parameters as described in Section 4.2. In order to isolate the parameter estimation error from the community detection misclustering error, we simulate networks with a single block so that we do not need to run spectral clustering. The rest of the base network’s parameters are as follows:  $T = 100$ ,  $\mu = 1.8$ ,  $\alpha = 7$ , and  $\beta = 8$ . For each value of  $n$ , we estimate all four aforementioned parameters using the procedure described in Section 3.2. Lastly, we measure mean-squared error (MSE) over 100 simulations.

As shown in Figure 6, the mean squared errors of all four estimators approach zero as  $n$  increases with shrinking standard errors across simulations. We proved the consistency of  $\hat{m}$  and  $\hat{\mu}$  estimators in Theorem 3 in Section 4.2 and predicted the mean-squared error to decrease at a quadratic rate. In this section we empirically validated our result in finite samples as it is depicted in Figures 6a and 6b. Moreover, since the estimation of  $\alpha$  and  $\beta$  depends on  $\hat{m}$  and  $\hat{\mu}$ , we empirically observe that accurate estimation of  $m$  and  $\mu$  leads to accurate estimation of  $\alpha$  and  $\beta$  as well (Figures 6c and 6d) even though  $\beta$  is estimated using a line search<sup>1</sup>.

## 5.2 Real Networks

We perform experiments on three real network datasets. Each dataset consists of a set of events where each event is denoted by a sender, a receiver, and a timestamp. The MIT Reality Mining and Enron datasets were loaded and preprocessed identically to DuBois et al. (2013) to allow for a fair comparison with their reported values.

- MIT Reality Mining (Eagle et al., 2009): Consists of 2,161 phone calls where the start time of each call was used as the event timestamp. This dataset has a “core-periphery” structure, where there is a core group for whom we have all of their communication data and a much larger group of people in the periphery who had contact with the core. We consider calls between pairs of the core 70 callers and recipients. The duration of the entire dataset was adjusted to  $[0, 1000]$ , and the last 661 phone calls were used as the test set<sup>2</sup>.
- Enron (Klimt and Yang, 2004): Consists of 4,000 emails exchanged among 142 individuals. Similarly, duration was adjusted to  $[0, 1000]$ , and the last 1,000 emails were held out as the test set.
- Facebook Wall Posts (Viswanath et al., 2009): Consists of a total of 876,993 wall posts from 46,952 users from September 2004 to January 2009. We consider only posts from a user to another user’s wall so that there are no self-edges. We analyze both the full data set and the same subset of this dataset that was used by Junuthula et al. (2019) consisting of 137,170 events, between January 1, 2007 to January 1, 2008,

---

1. The line search was performed using SciPy’s function `minimize_scalar(method="bounded")`: [https://docs.scipy.org/doc/scipy/reference/generated/scipy.optimize.minimize\\_scalar.html](https://docs.scipy.org/doc/scipy/reference/generated/scipy.optimize.minimize_scalar.html)

2. We found some inconsistencies between the actual dataset used and its description in DuBois et al. (2013). For a fair comparison, we loaded and preprocessed this dataset using their code available on GitHub: <https://github.com/doobwa/blockrem/blob/master/process/reality.r>.

Table 1: Comparison of the mean test log-likelihood per event for each real network dataset across all three models. Larger (less negative) values indicate a better fit. Dashes indicate values that were not reported (for REM) or required excessive computation time (for BHM).

Datasets & Models								
K	MIT Reality Mining			Enron			Facebook Wall Posts	
	CHIP	REM	BHM	CHIP	REM	BHM	CHIP	BHM
1	<b>-4.833</b>	-6.783	-9.051	-5.634	-7.025	-8.716	-9.383	-14.496
2	-4.914	-7.417	-7.558	<b>-5.589</b>	-6.860	-8.428	-9.387	-14.052
3	-5.016	-6.107	-7.781	-5.648	-6.835	-8.392	-9.380	-13.836
5	-6.409	–	-6.207	-6.319	–	-7.908	<b>-9.363</b>	–
8	-5.481	–	-5.889	-6.361	–	-7.488	-9.366	–
10	-5.898	-6.605	-5.831	-6.777	-7.264	-8.012	-9.368	–

among 3,582 nodes for comparison against their block Hawkes model. Converting the time units from seconds to hours and adjusting the first timestamp to start at time 0, resulted in a duration range of  $[0, 8759.9]$ . Lastly, the data set was divided into train and test using a 80/20 split on the number of events.

### 5.2.1 MODEL COMPARISON

We fit our proposed Community Hawkes Independent Pairs (CHIP) model as well as the Block Hawkes Model (BHM) (Junuthula et al., 2019) to all three real datasets and evaluate their fit. Since we do not have ground-truth community labels for these real datasets, we evaluate the goodness of fit using the log-likelihood on the test data in the same manner as in DuBois et al. (2013). We will also directly compare against the available results for the relational event model (REM) reported in DuBois et al. (2013). We note that since all the three models assume the same Poisson process for arrival of events with different rates (which are governed by different set of parameters), the joint distribution of event times has the same form for all three models. Hence the likelihood function of the models are directly comparable. Therefore, the test log-likelihood is a reasonable metric for comparing the fits of the models to the data.

First, we use the estimation procedure explained in Section 3.2 to estimate all CHIP’s Hawkes Process parameters using the training set (the entire dataset excluding the test set). Next, we calculate the model log-likelihood on the entire dataset and subtract the training log-likelihood from it. The result is then divided by the total number of events in the test set to evaluate the mean log-likelihood per test event, which is the metric used in DuBois et al. (2013). Lastly, if a node in the test set did not appear in the training data, it was automatically assigned to the largest block.

We implemented the BHM by using spectral clustering followed by local search, since it was shown by Junuthula et al. (2019) to achieve the highest adjusted Rand score in simulations compared to just spectral clustering and variational EM. For all datasets, we

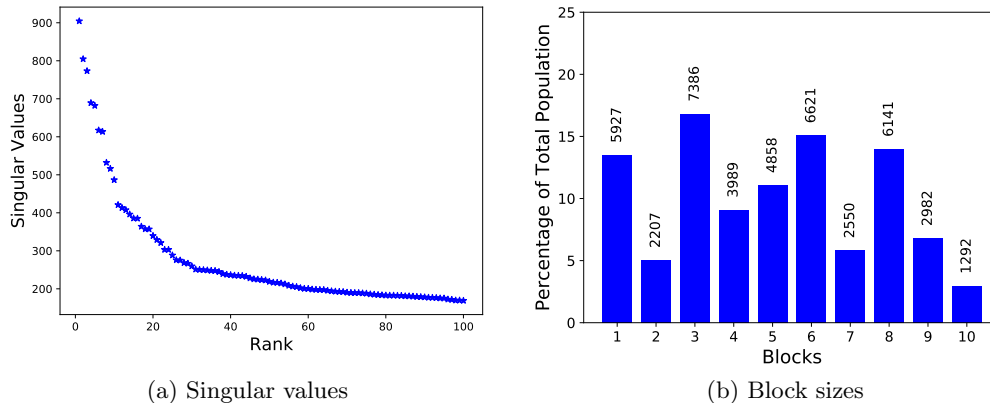


Figure 7: Results of spectral clustering on the weighted adjacency matrix of the largest connected component of the Facebook Wall Posts dataset. (a) 100 largest singular values. There is a large gap between the 10<sup>th</sup> and the 11<sup>th</sup> largest singular values that leads us to select  $k = 10$  blocks. (b) Size of each formed block. Numbers on top of each bar indicate the actual number of nodes in that block.

allowed local search to converge for all values of  $k$ ; however, for the Facebook Wall Posts data, we limited the model to  $k \leq 3$  due to the high computational time of the local search.

As shown in Table 1, CHIP outperforms all other models in all three datasets. In the MIT Reality Mining dataset, CHIP actually achieves the highest log-likelihood when there is no community structure ( $k = 1$ ). It is also worth noting that fitting CHIP for each value of  $k$  on average took about 0.15 s, 0.3 s, and 17 s on the MIT Reality Mining, Enron, and Facebook datasets, respectively, while the BHM on average took about 250 s, 30 m, and 44 h, mostly due to the time-consuming local search<sup>3</sup>. The results shown for REM are the reported values from DuBois et al. (2013). We did not implement their MCMC-based inference procedure and thus do not have results for REM on the Facebook data or computation times.

### 5.2.2 EXPLORATORY ANALYSIS OF THE FACEBOOK WALL POSTS DATASET USING CHIP

We further explore the fit and the scalability of our CHIP model by fitting it to the largest connected component of the entire Facebook Wall Posts dataset (excluding self loops), consisting of 43,953 nodes and 852,833 edges. Considering the gap between the 10<sup>th</sup> and the 11<sup>th</sup> largest singular values of the weighted adjacency matrix of the network as shown in Figure 7a, we choose a model with  $k = 10$  blocks, resulting in the block sizes depicted in Figure 7b. The entire model fitting procedure, as described in Algorithm 2, only took 141.4 s:

- Community detection by spectral clustering: 7.5 s.

3. All computations were done on a workstation with 2 Intel Xeon 2.3 GHz processors with a total of 36 physical cores and 256 GB of memory.

- Estimating  $m$  and  $\mu$  using (4) and (5), respectively: 28.6 s.
- Estimating  $\alpha$  and  $\beta$  using line search: 105.3 s.

This demonstrates the scalability of the CHIP model and the fact that it can be utilized to model much larger data sets. It is worth noting that the for-loop at line 5 of Algorithm 2, can be parallelized to drop the computational time even further for parameter estimation, although we did not do so due to the already low computation time.

Figure 8 shows heatmaps of the fitted CHIP parameters. The base intensity  $\mu$  of the wall posts (Figure 8a) tend to track the mean number of events per node pair (Figure 8f), as predicted by the asymptotic mean number of events between node pairs given in (8). Put another way, block pairs containing node pairs with frequent wall posts are modeled to have higher  $\mu$ 's. Moreover, diagonal block pairs on average have a base intensity of  $2.8 \times 10^{-7}$  which is higher compared to  $9.5 \times 10^{-8}$  for off-diagonal block pairs, indicating an underlying assortative community structure. Although diagonal block pairs have a higher base intensity on average, there are some off-diagonal block pairs with a high  $\mu$  such as (5, 8), (8, 5), and (6, 4), which illustrates that the CHIP model does not discourage inter-block events. These patterns often occur in social networks, for instance, if there are communities with opposite views on a particular subject.

While the structure of  $\mu$  reveals insights on the baseline rates of events between block pairs, the structure of  $\alpha$  (Figure 8c) and  $\beta$  (Figure 8d) reveal insights on the burstiness of events between block pairs. Note that the structure of the  $\alpha$  to  $\beta$  ratio  $m$  (Figure 8b) affects the asymptotic mean number of events in (8). For some block pairs, such as (3, 10), there are very low values of  $\alpha$  and  $\beta$  indicating the events are closely approximated by a homogeneous Poisson process. Notice that the difference between the base intensity,  $\mu$ , of block pair (5, 8) and the two block pairs (6, 9) and (6, 10) in Figure 8a is larger than the corresponding difference in their mean number of events in Figure 8f. This difference is accounted for by the burstiness of block pairs (6, 9) and (6, 10), with higher values of  $m$ , compared to (5, 8).

Another interesting observation is that almost all block pairs with a high  $\mu$  are accompanied by a high  $m$ . That is, block pairs with a high baseline rate of events also tend to be bursty. The reverse does not always hold. A high  $m$  either denotes a high  $\alpha$  or a low  $\beta$ ; in either case it results in a higher overall intensity once an event arrives, encouraging more events to occur. Thus, there are some block pairs, such as (2, 8) that have a low baseline rate of events but are extremely bursty, which relatively increases the mean number of events per node pair. The different levels of burstiness of block pairs cannot be seen from aggregate statistics such as the total number of events (Figure 8e) or even the mean number of events per node pair (Figure 8f).

Unlike the findings of Junuthula et al. (2019), who studied only a subset of the network containing 3,582 nodes using  $k = 2$  blocks, we find that  $\alpha$  is not necessarily higher for diagonal blocks as shown in Figure 8c. Even though we do not explicitly model reciprocity between node pairs in our CHIP model, we can nevertheless empirically observe certain reciprocities through the patterns of the estimated  $\alpha$  and  $\beta$  parameters. We note that the high reciprocity present in social networks is captured by CHIP through the symmetry in all Hawkes process parameters about block pairs. This can be observed in block pairs (8, 5) and (5, 8). In the context of this dataset, a symmetric  $\alpha$  and  $\beta$  corresponds to the notion



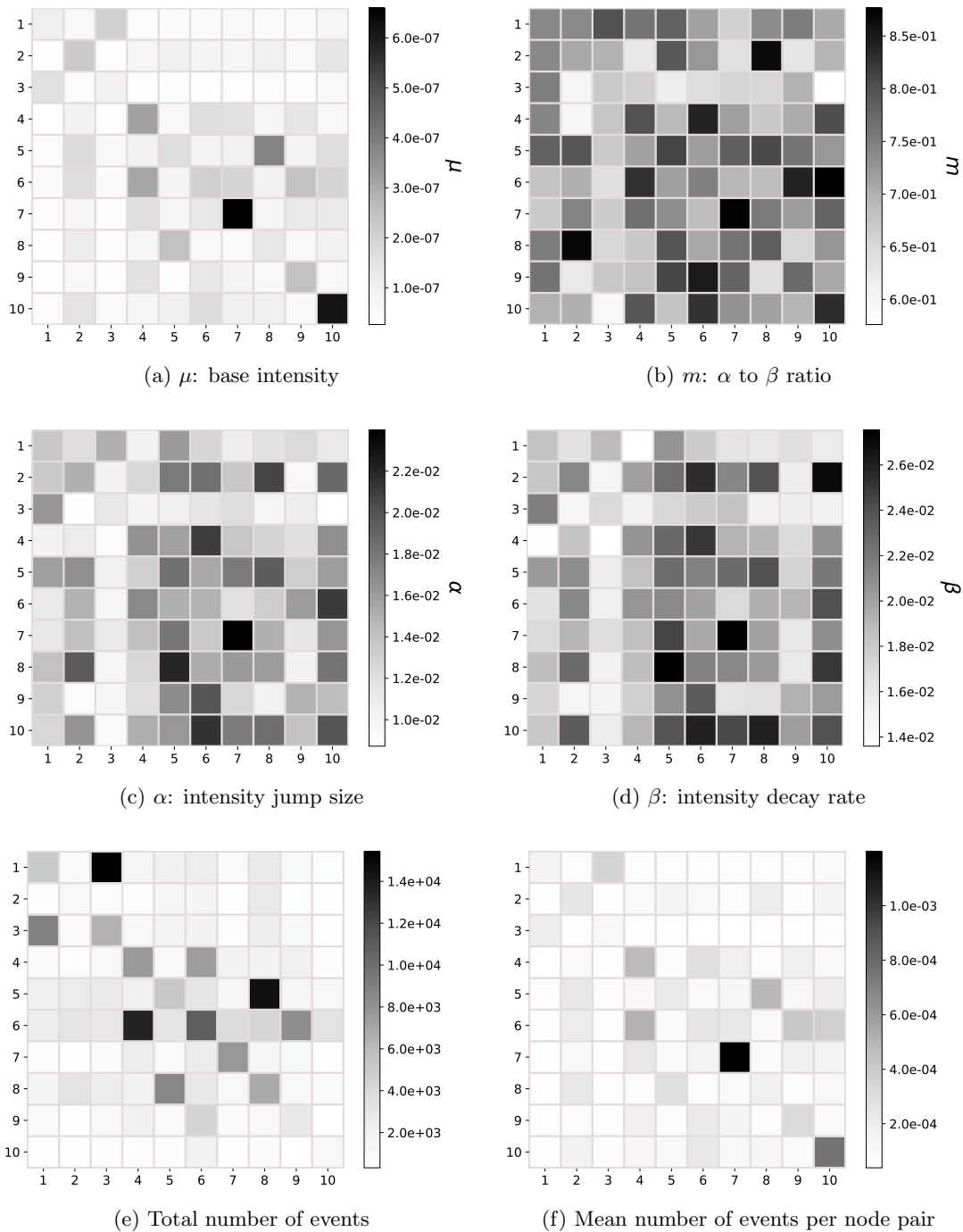


Figure 8: Inferred CHIP parameters on the largest connected component of the Facebook Wall Posts dataset with  $k = 10$ . Axis labels denote block numbers. Each tile corresponds to a block pair where  $(a, b)$  denotes row  $a$  and column  $b$ .

that wall posts posted by the people in block 5 on the wall of the people in block 8 will urge people in block 8 to respond, which in turn promotes more wall posts by people in block 5.

Lastly, it is worth noting that fitting the CHIP model to this data set using the unweighted adjacency matrix resulted in a per event log-likelihood of  $-10.04$  compared to  $-9.67$  for the weighted adjacency matrix on the test data set when using a 80/20 train and test split. Thus, this was another reason to use the weighted adjacency matrix besides its aforementioned advantages in previous sections. We note that running spectral clustering on the unweighted adjacency matrix, compared to the weighted adjacency matrix, seemed to detect communities with larger number of intra-block events, while inter-block events were a lot less common.

## 6. Conclusion

We introduced the Community Hawkes Independent Pairs (CHIP) model for community detection in continuous-time dynamic networks of relational events with timestamps. The CHIP model has many similarities with the Block Hawkes Model (BHM) recently proposed by Junuthula et al. (2019), both of which are motivated by the Stochastic Block model. However unlike the BHM, in the CHIP model, events among any two node pairs are independent which enables tractable analysis of the model. We demonstrated that spectral clustering on both the unweighted and weighted adjacency matrices constructed from the relational events provide consistent community detection for a growing number of nodes. We further discussed the pros and cons of using the weighted vs. unweighted adjacency matrix for spectral clustering in different settings accompanied by upper bounds for their misclustering error rates. We then proposed a computationally efficient and consistent estimator for two of the Hawkes process parameters for a growing number of nodes and time duration. Lastly, we showed that CHIP not only provides better fits to several real-world relational events data sets compared to the Relational Event Model (DuBois et al., 2013) and the BHM, but that it is also computationally more efficient. That enables our proposed CHIP model to scale to considerably larger data sets, including a Facebook wall post network with over 40,000 nodes and 800,000 events.

## Acknowledgments

This material is based upon work supported by the National Science Foundation grants DMS-1830412 and IIS-1755824.

## Appendix A. Proofs

We present proofs of our results for estimated community assignments presented in Section 4.1 followed by proofs of our results for estimated Hawkes process parameters presented in Section 4.2.

### A.1 Estimated Community Assignments

We begin with the proof of Theorem 1 for the estimated community assignments from the unweighted adjacency matrix.

PROOF OF THEOREM 1

**Proof**

We note that the matrix  $A$  is an adjacency matrix with independent entries. Further  $n \max_{ij} E[A_{ij}] \leq \Delta$  and  $\Delta \geq c_0 \log n$  by definition. Then by Theorem 5.2 of Lei and Rinaldo (2015), we have with probability at least  $1 - n^{-r}$ ,

$$\|A - E[A]\|_2 \leq c\sqrt{\Delta}, \quad (15)$$

where  $c$  is a constant dependent on  $c_0$  and  $r$ .

Since  $E[A]$  can be written in the form of a stochastic block model as  $E[A] = C(1 - \exp(-\mu T))C^T$ , we can use known results in the SBM literature. Let  $\hat{U}_{n \times k}$  denote the  $n \times k$  matrix whose columns are the top  $k$  eigenvectors of the matrix  $A$ . By Lemma 3.1 of Rohe et al. (2011), the matrix of eigenvectors corresponding to the largest  $k$  non-zero eigenvalues of the matrix  $E[A]$  is  $C(C^T C)^{-1/2} \mathcal{O}$  for some  $k \times k$  orthogonal matrix  $\mathcal{O}$ . Then we have the following relationship for the difference between matrices of population eigenvectors (those of  $E[A]$ ) and sample eigenvectors (those of  $A$ ) and the misclustering error rate of community detection by applying  $(1 + \epsilon)$  approximate  $k$ -means algorithm to those matrices (Pensky et al., 2019):

$$r \leq \frac{1}{n} |a|_{\max} 8(2 + \epsilon) \|\hat{U} - C(C^T C)^{-1/2} \mathcal{O}\|_F^2. \quad (16)$$

Next we use the celebrated Davis-Kahan Theorem (Davis and Kahan, 1970; Stewart and Sun, 1990) that relates perturbation of matrices to perturbation of eigenspaces of those matrices. Then we have the following bound on the misclustering rate (also see Lemma 5.1 of Lei and Rinaldo (2015)):

$$r \leq \frac{1}{n} |a|_{\max} 8(2 + \epsilon) \|\hat{U} - C(C^T C)^{-1/2} \mathcal{O}\|_F^2 \leq 64(2 + \epsilon) \frac{|a|_{\max} k \|A - E[A]\|_2^2}{n(\lambda_{\min}(E[A]))^2}. \quad (17)$$

Combining (15) and (17), we arrive at the desired result. ■

PROOF OF THEOREM 2

**Proof** We start with the following result.

**Lemma 1** *Let  $Y$  be a relational event matrix on  $n$  nodes generated according to a  $k$ -block CHIP model with community assignment matrix  $C$  and parameter matrices  $\mu, \alpha, \beta$ . Let  $N$  be the weighted adjacency matrix obtained by aggregating  $N$  at time  $T$ . Then with probability at least  $1 - 1/n$ , we have*

$$\|N - E[N]\|_2 \leq (1 + \epsilon) \left\{ 2s + \frac{6}{\log(1 + \epsilon)} s_1 \sqrt{\log n} \right\} + 2s_1 \sqrt{\log n}, \quad (18)$$

where  $0 < \epsilon < 1/2$  is a constant, and the terms  $s$  and  $s_1$  are as defined in (10) and (11), respectively.

We present the proof of this lemma following the proof of Corollary 2.

Since  $E[N]$  can also be written in the form of a stochastic block model as  $E[N] = C\nu C^T$ , we can use the same arguments as in the proof of the previous result. Using the Davis-Kahan Theorem (Davis and Kahan, 1970; Stewart and Sun, 1990), we have the following bound:

$$r \leq \frac{1}{n} |a|_{\max} 8(2 + \epsilon_1) \|\hat{U} - C(C^T C)^{-1/2} \mathcal{O}\|_F^2 \leq 64(2 + \epsilon_1) \frac{|a|_{\max} k \|N - E[N]\|_2^2}{n(\lambda_{\min}(E[N]))^2}, \quad (19)$$

Combining (18) and (19), we arrive at the desired result. ■

Next, we present the proofs of the corollaries for the simplified special case with  $k$  equivalent communities.

#### PROOF OF COROLLARY 1

**Proof** Under the simplified model all communities have the same number of nodes, i.e.,  $|a| = \frac{n}{k}$  for all  $a$ , and consequently  $|a|_{\max} = \frac{n}{k}$ . Further, we can write

$$E[A] = C \left( (\exp(-\mu_2 T) - \exp(-\mu_1 T)) I_k + (1 - \exp(-\mu_2 T)) \mathbf{1}_k \mathbf{1}_k^T \right) C^T,$$

where  $I_k$  is the  $k$ -dimensional identity matrix, and  $\mathbf{1}_k$  is the  $k$ -dimensional vector of all 1's. Then by Rohe et al. (2011),  $\mathbf{1}_k$  is an eigenvector corresponding to the eigenvalue  $\frac{n}{k}(\exp(-\mu_2 T) - \exp(-\mu_1 T)) + n(1 - \exp(-\mu_2 T))$ , and the remaining non-zero eigenvalues are of the form  $\frac{n}{k}(\exp(-\mu_2 T) - \exp(-\mu_1 T))$ . Since  $n(1 - \exp(-\mu_2 T)) > 0$ , the smallest in absolute value non-zero eigenvalue of  $E[A]$  is then,

$$\lambda_{\min}(E[A]) = \frac{n}{k}(\exp(-\mu_2 T) - \exp(-\mu_1 T)).$$

Also, under this setting, the numerator in the upper bound from Theorem 1 becomes

$$\Delta = n(1 - \exp(-\mu_1 T)).$$

Substituting these quantities into (7), we arrive at (13), the first statement of the corollary.

If we further assume that  $\mu T$  is small then we can make some further simplifications using the Taylor series expansion of  $\exp(-x)$  near  $x = 0$ . In this case,

$$\lambda_{\min} \asymp \frac{n}{k}(\mu_1 - \mu_2)T,$$

and

$$\Delta \asymp n\mu_1 T.$$

Substituting these quantities into (7), we arrive at (14), the second statement of the corollary, which completes the proof. ■

## PROOF OF COROLLARY 2

**Proof** Under the simplified model we have

$$E[N] = C \left( (\nu_1 - \nu_2) T I_k + \nu_2 T \mathbf{1}_k \mathbf{1}_k^T \right) C^T.$$

As before all communities have the same number of nodes, i.e.,  $|a| = \frac{n}{k}$  for all  $a$ , and  $|a|_{\max} = \frac{n}{k}$ . Then by Rohe et al. (2011),  $\mathbf{1}_k$  is an eigenvector corresponding to the eigenvalue  $\frac{n}{k}(\nu_1 - \nu_2)T + n\nu_2T$ , and the remaining non-zero eigenvalues are of the form  $\frac{n}{k}(\nu_1 - \nu_2)T$ . Since  $n\nu_2 > 0$ , the smallest non-zero eigenvalue

$$\lambda_{\min}(E[N]) = \frac{n}{k}(\nu_1 - \nu_2)T.$$

The upper bound from Theorem 2 can also be simplified further under this model. We have

$$s = \sqrt{T} \sqrt{\frac{n}{k} \sigma_1^2 + \frac{(k-1)n}{k} \sigma_2^2} \asymp \sqrt{\frac{nT}{k}} \sqrt{\sigma_1^2 + (k-1)\sigma_2^2} \asymp \sqrt{nT} \sigma_1,$$

and

$$s_1 = \sqrt{T} \sigma_1,$$

and consequently,

$$(1 + \epsilon) \left( 2s + \frac{6}{\log(1 + \epsilon)} s_1 \sqrt{\log n} \right) + 2s_1 \sqrt{\log n} \asymp \sqrt{T} \sigma_1 \left( \sqrt{n} + \sqrt{\log n} \right) \lesssim \sqrt{T} \sigma_1 \sqrt{n}.$$

Substituting these quantities into (12) completes the proof. ■

## PROOF OF LEMMA 1

**Proof** We note that  $N_{ij}$  is asymptotically normal (Theorem 4 of Hawkes and Oakes (1974)) as  $T \rightarrow \infty$ , i.e.

$$N_{ij} | (C_{ia} = 1, C_{jb} = 1) \sim \mathcal{N}(\nu_{ab}, \sigma_{ab}^2).$$

Then  $(N - E[N])$  is a  $n \times n$  symmetric matrix with elements  $(N - E[N])_{ij} = g_{ij} \sigma_{ij}$ , where  $g_{ij}; i \geq j$  are i.i.d  $\mathcal{N}(0, 1)$  and  $\sigma_{ij}$  is the standard deviation of  $N_{ij}$  given before.

We will use Corollary 3.9 in Bandeira et al. (2016). In the notation of Bandeira et al. (2016), we set  $\sigma = s$ ,  $\sigma^* = s_1$  and let  $t = 2s_1 \sqrt{\log n}$ . Then for any  $0 < \epsilon < 1/2$ , we have

$$P \left( \|N - E[N]\|_2 \geq (1 + \epsilon) \left\{ 2s + \frac{6}{\log(1 + \epsilon)} s_1 \sqrt{\log n} \right\} + 2s_1 \sqrt{\log n} \right) \leq \exp(-\log n). ■$$

## A.2 Estimated Hawkes Process Parameters

### PROOF OF THEOREM 3

**Proof** First, using the Central Limit Theorem and Law of Large Numbers, we have

$$\bar{N}_{ab} \xrightarrow{d} \mathcal{N}\left(\nu_{ab}, \frac{\sigma_{ab}^2}{n_{ab}}\right) \text{ and } S_{ab}^2 \xrightarrow{p} \sigma_{ab}^2, \quad \text{as } n_{ab} \rightarrow \infty.$$

Then by Slutsky's theorem (Lehmann, 2004) we have,

$$\frac{\bar{N}_{ab}}{S_{ab}^2} \xrightarrow{d} \mathcal{N}\left(\frac{\nu_{ab}}{\sigma_{ab}^2}, \frac{1}{\sigma_{ab}^2 n_{ab}}\right) \Leftrightarrow \sqrt{n_{ab}} \left(\frac{\bar{N}_{ab}}{S_{ab}^2} - \frac{\nu_{ab}}{\sigma_{ab}^2}\right) \xrightarrow{d} \mathcal{N}\left(0, \frac{1}{\sigma_{ab}^2}\right).$$

Finally, we will apply the delta method (See Theorem 2.5.2 of Lehmann (2004)) on the random variable  $X = \frac{\bar{N}_{ab}}{S_{ab}^2}$  with the function  $g(x) = 1 - \sqrt{x}$ . Note that  $g'(x) = \frac{1}{2\sqrt{x}}$ . Then we can compute  $g'\left(\frac{\nu_{ab}}{\sigma_{ab}^2}\right) = \frac{\sigma_{ab}}{2\sqrt{\nu_{ab}}}$ . Then we have

$$\sqrt{n_{ab}} \left(\hat{n}_{ab} - \left(1 - \sqrt{\frac{\nu_{ab}}{\sigma_{ab}^2}}\right)\right) \xrightarrow{d} \mathcal{N}\left(0, \frac{1}{4\nu_{ab}}\right).$$

Next we derive the asymptotic distribution for  $\hat{\mu}_{ab}$ . We first apply the delta method to the random variable  $\bar{N}_{ab}$  with the function  $g(x) = x^{3/2}$ . Clearly,  $g'(x) = \frac{3}{2}\sqrt{x}$ , such that  $g'(\nu_{ab}) = \frac{3}{2}\sqrt{\nu_{ab}}$ . Then we have

$$\sqrt{n_{ab}}((\bar{N}_{ab})^{3/2} - (\nu_{ab})^{3/2}) \xrightarrow{d} \mathcal{N}\left(0, \frac{9}{4}\nu_{ab}\sigma_{ab}^2\right).$$

Applying Slutsky's theorem, we then have

$$\sqrt{n_{ab}} \left(\frac{(\bar{N}_{ab})^{3/2}}{S_{ab}} - \frac{(\nu_{ab})^{3/2}}{\sigma_{ab}}\right) \xrightarrow{d} \mathcal{N}\left(0, \frac{9}{4}\nu_{ab}\right).$$

■

## References

Emmanuel Abbe. Community detection and stochastic block models: recent developments. *The Journal of Machine Learning Research*, 18(1):6446–6531, 2017.

Emmanuel Abbe and Colin Sandon. Community detection in general stochastic block models: Fundamental limits and efficient algorithms for recovery. In *IEEE 56th Annual Symposium on Foundations of Computer Science (FOCS)*, pages 670–688. IEEE, 2015.

Emmanuel Bacry, Iacopo Mastromatteo, and Jean-François Muzy. Hawkes processes in finance. *Market Microstructure and Liquidity*, 1(01):1550005, 2015.

- Emmanuel Bacry, Stéphane Gaïffas, Iacopo Mastromatteo, and Jean-François Muzy. Mean-field inference of hawkes point processes. *Journal of Physics A: Mathematical and Theoretical*, 49(17):174006, 2016.
- Emmanuel Bacry, Martin Bompaire, Philip Deegan, Stéphane Gaïffas, and Søren V Poulsen. Tick: a python library for statistical learning, with an emphasis on hawkes processes and time-dependent models. *The Journal of Machine Learning Research*, 18(1):7937–7941, 2017.
- Afonso S Bandeira, Ramon Van Handel, et al. Sharp nonasymptotic bounds on the norm of random matrices with independent entries. *The Annals of Probability*, 44(4):2479–2506, 2016.
- Sharmodeep Bhattacharyya and Shirshendu Chatterjee. Spectral clustering for multiple sparse networks: I. *arXiv preprint arXiv:1805.10594*, 2018.
- Charles Blundell, Jeff Beck, and Katherine A. Heller. Modelling reciprocating relationships with Hawkes processes. In *Advances in Neural Information Processing Systems 25*, pages 2600–2608, 2012.
- Peter Chin, Anup Rao, and Van Vu. Stochastic block model and community detection in sparse graphs: A spectral algorithm with optimal rate of recovery. In *COLT*, pages 391–423, 2015.
- José Da Fonseca and Riadh Zaatour. Hawkes process: Fast calibration, application to trade clustering, and diffusive limit. *Journal of Futures Markets*, 34(6):548–579, 2014.
- Chandler Davis and William Morton Kahan. The rotation of eigenvectors by a perturbation. iii. *SIAM Journal on Numerical Analysis*, 7(1):1–46, 1970.
- Andrew Daw and Jamol Pender. Queues driven by hawkes processes. *Stochastic Systems*, 8(3):192–229, 2018.
- Christopher DuBois and Padhraic Smyth. Modeling relational events via latent classes. In *Proceedings of the 16th ACM SIGKDD International Conference on Knowledge Discovery and Data Mining*, pages 803–812, 2010.
- Christopher DuBois, Carter T. Butts, and Padhraic Smyth. Stochastic blockmodeling of relational event dynamics. In *Proceedings of the 16th International Conference on Artificial Intelligence and Statistics*, pages 238–246, 2013.
- Nathan Eagle, Alex Sandy Pentland, and David Lazer. Inferring friendship network structure by using mobile phone data. *Proceedings of the national academy of sciences*, 106(36):15274–15278, 2009.
- Paul Embrechts, Thomas Liniger, and Lu Lin. Multivariate hawkes processes: an application to financial data. *Journal of Applied Probability*, 48(A):367–378, 2011.

- Mehrdad Farajtabar, Yichen Wang, Manuel Gomez Rodriguez, Shuang Li, Hongyuan Zha, and Le Song. COEVOLVE: A joint point process model for information diffusion and network co-evolution. In *Advances in Neural Information Processing Systems 28*, pages 1945–1953, 2015.
- Eric W. Fox, Martin B. Short, Frederic P. Schoenberg, Kathryn D. Coronges, and Andrea L. Bertozzi. Modeling e-mail networks and inferring leadership using self-exciting point processes. *Journal of the American Statistical Association*, 111(514):564–584, 2016.
- Chao Gao, Zongming Ma, Anderson Y Zhang, and Harrison H Zhou. Achieving optimal misclassification proportion in stochastic block models. *The Journal of Machine Learning Research*, 18(1):1980–2024, 2017.
- Anna Goldenberg, Alice X Zheng, Stephen E Fienberg, Edoardo M Airoldi, et al. A survey of statistical network models. *Foundations and Trends in Machine Learning*, 2(2):129–233, 2010.
- Eric C. Hall and Rebecca M. Willett. Tracking dynamic point processes on networks. *IEEE Transactions on Information Theory*, 62(7):4327–4346, 2016.
- Peter F Halpin and Paul De Boeck. Modelling dyadic interaction with hawkes processes. *Psychometrika*, 78(4):793–814, 2013.
- Alan G Hawkes. Point spectra of some mutually exciting point processes. *Journal of the Royal Statistical Society. Series B (Methodological)*, pages 438–443, 1971a.
- Alan G Hawkes. Spectra of some self-exciting and mutually exciting point processes. *Biometrika*, 58(1):83–90, 1971b.
- Alan G Hawkes and David Oakes. A cluster process representation of a self-exciting process. *Journal of Applied Probability*, 11(3):493–503, 1974.
- Xinran He, Theodoros Rekatsinas, James Foulds, Lise Getoor, and Yan Liu. HawkesTopic: A joint model for network inference and topic modeling from text-based cascades. In *Proceedings of the 32nd International Conference on Machine Learning*, pages 871–880, 2015.
- P. D. Hoff, A. E. Raftery, and M. S. Handcock. Latent space approaches to social network analysis. *J. Amer. Statist. Assoc.*, 97:1090–1098, 2002.
- Paul W Holland, Kathryn Blackmond Laskey, and Samuel Leinhardt. Stochastic blockmodels: First steps. *Social networks*, 5(2):109–137, 1983.
- Lawrence Hubert and Phipps Arabie. Comparing partitions. *Journal of Classification*, 2: 193–218, 1985.
- Ruthwik R. Junuthula, Maysam Haghdan, Kevin S. Xu, and Vijay K. Devabhaktuni. The Block Point Process Model for continuous-time event-based dynamic networks. In *Proceedings of the World Wide Web Conference*, pages 829–839, 2019.



- Bryan Klimt and Yiming Yang. The enron corpus: A new dataset for email classification research. In *European Conference on Machine Learning*, pages 217–226. Springer, 2004.
- Amit Kumar, Yogish Sabharwal, and Sandeep Sen. A simple linear time  $(1+\epsilon)$ -approximation algorithm for k-means clustering in any dimensions. In *In Proceedings of the 45th Annual IEEE Symposium on Foundations of Computer Science*, pages 454–462. IEEE, 2004.
- Patrick J Laub, Thomas Taimre, and Philip K Pollett. Hawkes processes. *arXiv preprint arXiv:1507.02822*, 2015.
- Erich Leo Lehmann. *Elements of large-sample theory*. Springer Science & Business Media, 2004.
- Jing Lei and Alessandro Rinaldo. Consistency of spectral clustering in stochastic block models. *The Annals of Statistics*, 43(1):215–237, 2015.
- P.A.W Lewis. Asymptotic properties and equilibrium conditions for branching poisson processes. *Journal of Applied Probability*, 6(2):355–371, 1969.
- Scott W. Linderman and Ryan P. Adams. Discovering latent network structure in point process data. In *Proceedings of the 31st International Conference on Machine Learning*, pages 1413–1421, 2014.
- Scott W. Linderman and Ryan P. Adams. Scalable Bayesian inference for excitatory point process networks. *arXiv preprint arXiv:1507.03228*, 2015. URL <https://arxiv.org/abs/1507.03228>.
- David Marsan and Olivier Lengline. Extending earthquakes’ reach through cascading. *Science*, 319(5866):1076–1079, 2008.
- Naoki Masuda, Taro Takaguchi, Nobuo Sato, and Kazuo Yano. Self-exciting point process modeling of conversation event sequences. In *Temporal Networks*, pages 245–264. Springer, 2013.
- Catherine Matias and Vincent Miele. Statistical clustering of temporal networks through a dynamic stochastic block model. *Journal of the Royal Statistical Society: Series B (Statistical Methodology)*, 79(4):1119–1141, 2017.
- Catherine Matias, Tabea Rebafka, and Fanny Villers. A semiparametric extension of the stochastic block model for longitudinal networks. *Biometrika*, 105(3):665–680, 2018.
- Jorge Nocedal and Stephen Wright. *Numerical optimization*. Springer Science & Business Media, 2006.
- Tohru Ozaki. Maximum likelihood estimation of hawkes’ self-exciting point processes. *Annals of the Institute of Statistical Mathematics*, 31(1):145–155, 1979.
- Subhadeep Paul and Yuguo Chen. Spectral and matrix factorization methods for consistent community detection in multi-layer networks. *arXiv Preprint arXiv:1704.07353*, 2017.

- Marianna Pensky, Teng Zhang, et al. Spectral clustering in the dynamic stochastic block model. *Electronic Journal of Statistics*, 13(1):678–709, 2019.
- Tai Qin and Karl Rohe. Regularized spectral clustering under the degree-corrected stochastic blockmodel. In *Advances in Neural Information Processing Systems 26*, pages 3120–3128, 2013.
- Marian-Andrei RizoIU, Lexing Xie, Scott Sanner, Manuel Cebrian, Honglin Yu, and Pascal Van Hentenryck. Expecting to be hip: Hawkes intensity processes for social media popularity. In *Proceedings of the 26th International Conference on World Wide Web*, pages 735–744. International World Wide Web Conferences Steering Committee, 2017.
- K. Rohe, S. Chatterjee, and B. Yu. Spectral clustering and the high-dimensional stochastic blockmodel. *Ann. Statist.*, 39(4):1878–1915, 2011.
- Aleksandr Simma and Michael I Jordan. Modeling events with cascades of poisson processes. *arXiv preprint arXiv:1203.3516*, 2012.
- Gilbert W Stewart and Ji-Guang Sun. *Matrix Perturbation Theory*. Academic Press, Boston, MA., 1990.
- Daniel L. Sussman, Minh Tang, Donniell E. Fishkind, and Carey E. Priebe. A consistent adjacency spectral embedding for stochastic blockmodel graphs. *Journal of the American Statistical Association*, 107(499):1119–1128, 2012.
- Long Tran, Mehrdad Farajtabar, Le Song, and Hongyuan Zha. NetCodec: Community detection from individual activities. In *Proceedings of the SIAM International Conference on Data Mining*, pages 91–99, 2015.
- Bimal Viswanath, Alan Mislove, Meeyoung Cha, and Krishna P Gummadi. On the evolution of user interaction in facebook. In *Proceedings of the 2nd ACM workshop on Online social networks*, pages 37–42. ACM, 2009.
- Ulrike Von Luxburg. A tutorial on spectral clustering. *Statistics and computing*, 17(4):395–416, 2007.
- Van Vu. A simple svd algorithm for finding hidden partitions. *Combinatorics, Probability and Computing*, 27(1):124–140, 2018.
- Lu Xin, Mu Zhu, and Hugh Chipman. A continuous-time stochastic block model for basketball networks. *The Annals of Applied Statistics*, 11(2):553–597, 2017.
- Eric P. Xing, Wenjie Fu, and Le Song. A state-space mixed membership blockmodel for dynamic network tomography. *The Annals of Applied Statistics*, 4:535–566, 2010.
- Kevin S. Xu. Stochastic block transition models for dynamic networks. In *Proceedings of the 18th International Conference on Artificial Intelligence and Statistics*, pages 1079–1087, 2015.

- Kevin S. Xu and Alfred O. Hero III. Dynamic stochastic blockmodels for time-evolving social networks. *IEEE Journal of Selected Topics in Signal Processing*, 8(4):552–562, 2014.
- Jiasen Yang, Vinayak Rao, and Jennifer Neville. Decoupling Homophily and Reciprocity with Latent Space Network Models. In *Proceedings of the Conference on Uncertainty in Artificial Intelligence*, 2017.
- Tianbao Yang, Yun Chi, Shenghuo Zhu, Yihong Gong, and Rong Jin. Detecting communities and their evolutions in dynamic social networks—a Bayesian approach. *Machine Learning*, 82(2):157–189, 2011.
- Qingyuan Zhao, Murat A Erdogdu, Hera Y He, Anand Rajaraman, and Jure Leskovec. Seismic: A self-exciting point process model for predicting tweet popularity. In *Proceedings of the 21th ACM SIGKDD International Conference on Knowledge Discovery and Data Mining*, pages 1513–1522. ACM, 2015.
- Ke Zhou, Hongyuan Zha, and Le Song. Learning triggering kernels for multi-dimensional hawkes processes. In *International Conference on Machine Learning*, pages 1301–1309, 2013.